Polarisation effects on the H-bond acceptor properties of sulfonamides

Fergal E. Hanna and Christopher A. Hunter*

Yusuf Hamied Department of Chemistry, University of Cambridge, Lensfield Road, Cambridge CB2 1EW, UK.

E-mail: herchelsmith.orgchem@ch.cam.ac.uk

Supplementary Information

Table of Contents

Materials and methods

All reagents were purchased from commercial sources (Sigma Aldrich UK, Acros, Tokyo Chemical Industry, Alfa Aesar and FluoroChem) and were used as received without any further purification unless stated. Dry solvents were obtained by means of a Grubbs solvent purification system.

Flash chromatography was done with an automated system (Combiflash Companion) using pre-packed cartridges of silica (50 µm PuriFlash® column) or basic alumina (45 µm PuriFlash® column)

The LC-MS analysis of samples was performed using Waters Acquity H-class UPLC coupled with a single quadrupole Waters SQD2. ACQUITY UPLC CSH C18 Column, 130 Å, 1.7 µm, 2.1 mm X 50 mm was used as the UPLC column for all samples. The conditions of the UPLC method are as follows: Solvent A: Water +0.1% Formic acid; Solvent B: Acetonitrile +0.1% Formic acid; Gradient of 0-2 minutes 5% - 100%B + 1 minute 100% B with re-equilibration time of 2 minutes. Flow rate: 0.6 ml/min; column temperature of 40°C; injection volume of 2 µL. The signal was monitored with MS-ES+, MS-ES-, and UV-vis absorption at 254 nm or at 290 nm.

^{1}H-NMR and ^{13}C-NMR were recorded on either a 400 MHz, 500 MHz or 700 MHz Bruker spectrometer. The reference values used for the chemical shifts of the various spectra are reported in the literature.[1] The splitting pattern is indicated with the following abbreviations: s for singlet, d for doublet, t for triplet, q for quartet, p for pentet and m for multiplet.

FT-IR spectra were collected with a Bruker ALPHA FT-IR Spectrometer.

UV-vis spectra were recorded with an Agilent UV-vis Cary 60 spectrophotometer.

Synthesis and characterisation

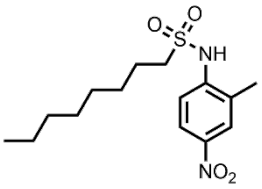

N-(2-methyl-4-nitrophenyl)octane-1-sulfonamide, **1**. 4-nitro-2-methylaniline (320 mg, 2.10 mmol) was dissolved in dry DCM (5 mL) under a nitrogen atmosphere. Pyridine (0.20 mL, 2.5 mmol) and 1-octanesulfonyl chloride (0.50 mL, 2.2 mmol) were added and the reaction stirred for 6 hours. The reaction mixture was quenched with HCl (1 M, 10 mL). The mixture was then extracted with DCM (3 x 10 mL) and the combined organics washed with brine (10 mL). The organic layer was dried with $MgSO_4$, and the solvent removed under reduced pressure. The crude residue was purified using flash chromatography (PE/EtOAc on SiO_2) to yield the desired product as a yellow crystalline solid (251 mg, 0.764 mmol, 36%)

m.p. – 132 – 133 °C

ν_{max} (film) cm^{-1} : 3298 (N-H), 2924 (C-H), 2854 (C-H), 1589 (C=C), 1519 (C=C), 1489 (C=C), 1410, 1335, 1149, 1135, 1097, 935, 904.

^1H NMR (400 MHz, $CDCl_3$) δ_H ppm: 8.09 (dd, J = 6.4, 2.8 Hz, 2H), 7.71 – 7.62 (m, 1H), 6.79 (s, 1H), 3.28 – 3.15 (m, 2H), 2.37 (s, 3H), 1.88 – 1.76 (m, 2H), 1.39 (q, J = 7.3 Hz, 2H), 1.25 (hd, J = 9.5, 8.4, 4.3 Hz, 9H), 0.85 (t, J = 6.8 Hz, 3H).

$^{13}C\{^1H\}$ NMR (101 MHz, $CDCl_3$) δ_C ppm: 143.7, 141.6, 127.2, 126.6, 123.4, 117.7, 53.0, 31.8, 29.1, 29.0, 28.2, 23.6, 22.7, 18.0, 14.2.

HRMS: calc for $C_{15}H_{23}N_2O_4S^-$ $[M-H]^-$: 327.1379, found: 317.1390.

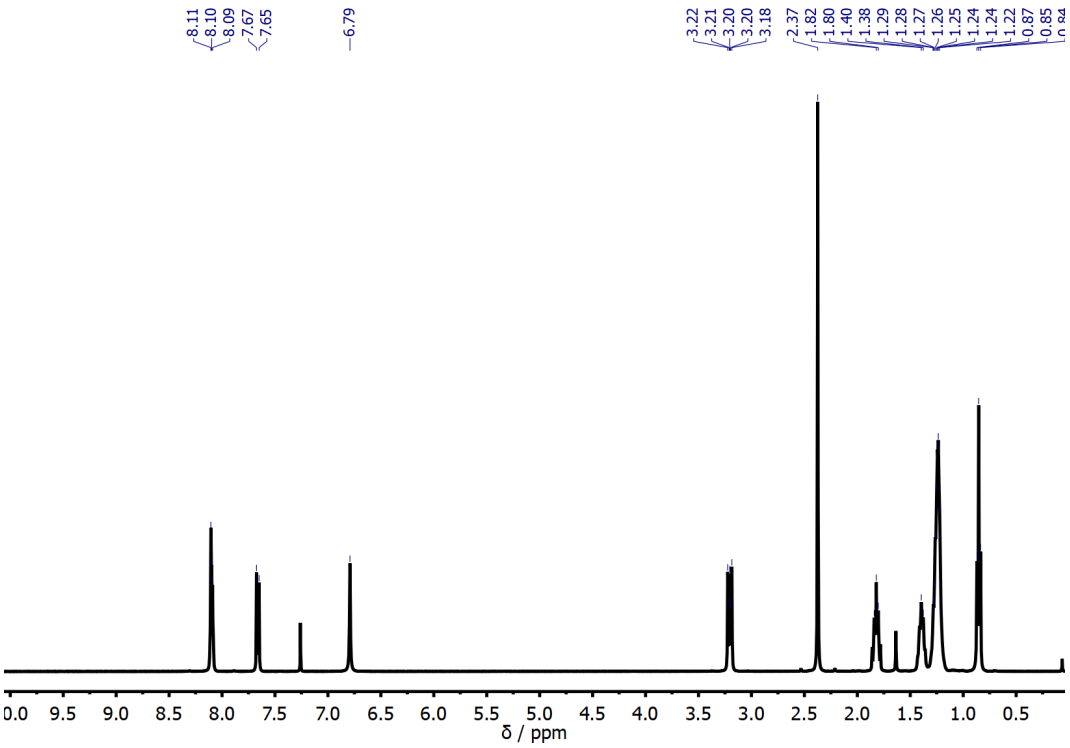

Figure S.1 – ^1H NMR spectrum of **1** in $CDCl_3$ (δ 0 – 10 ppm).

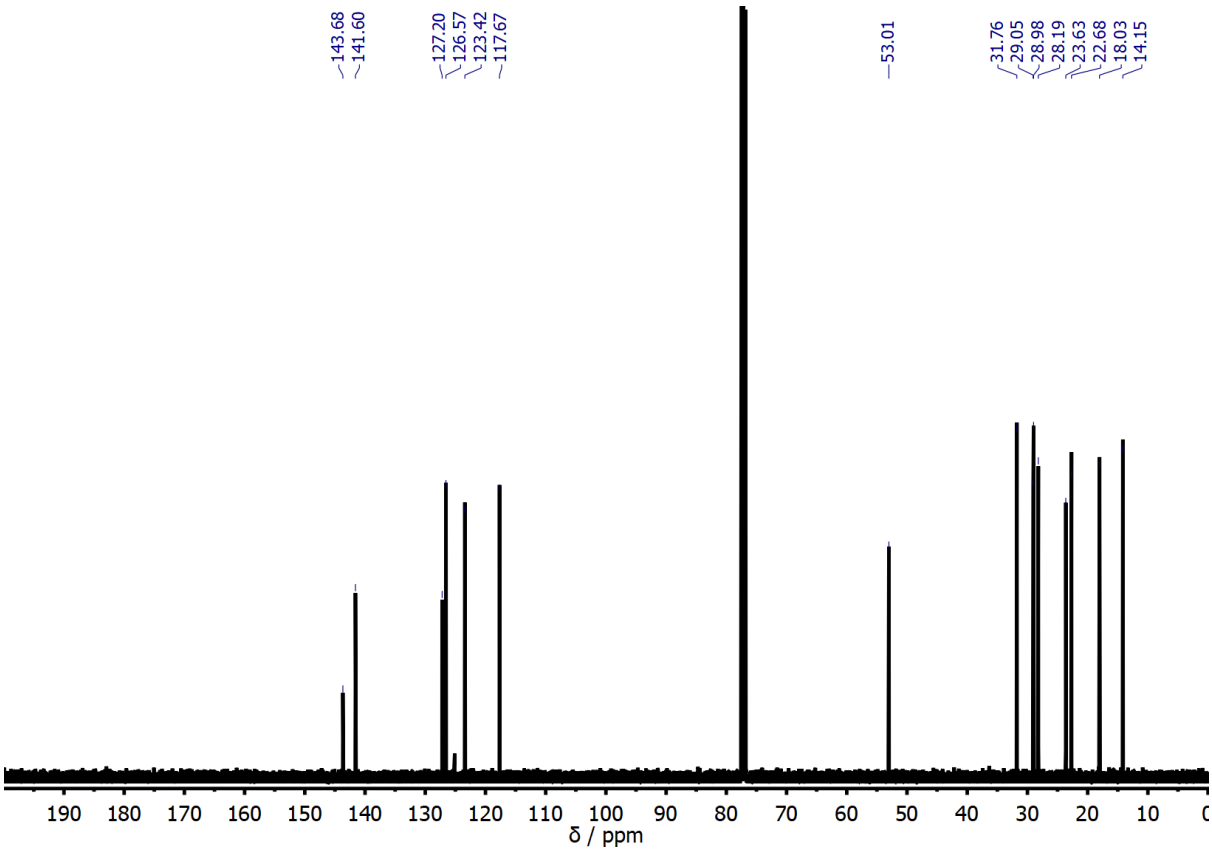

Figure S.2 – ^{13}C NMR spectrum of **1** in $CDCl_3$ (δ 0 – 200 ppm).

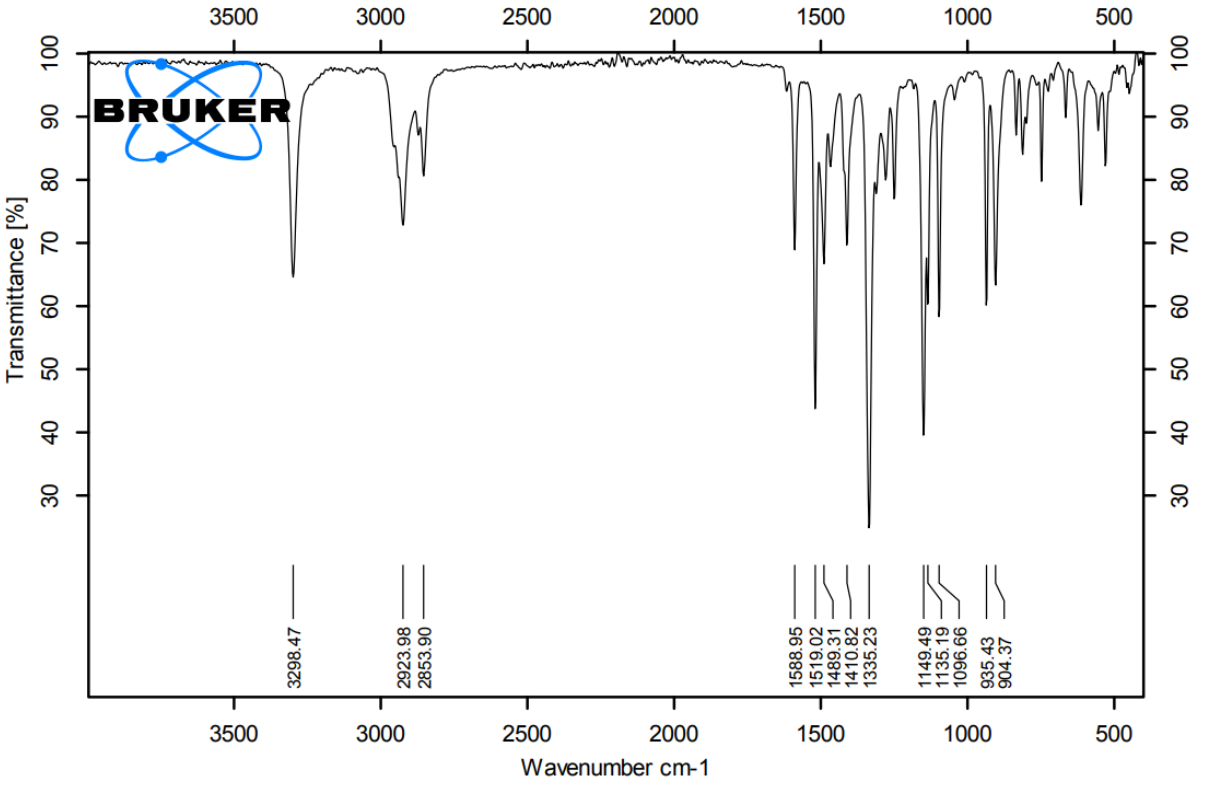

Figure S.3 – FT-IR spectrum of **1**.

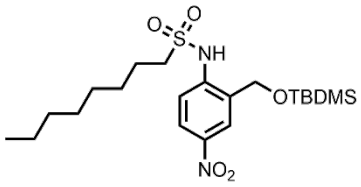

N-(2-(((tert-butyldimethylsilyl)oxy)methyl)-4-nitrophenyl)octane-1-sulfonamide, **2**. 2-(((*tert*-butyldimethylsilyl)oxy)methyl)-4-nitroaniline (0.487 g, 1.72 mmol) was dissolved in dry DCM (4 mL). Pyridine (0.15 mL, 1.86 mmol) and 1-octane sulfonyl chloride (0.40 mL, 1.73 mmol) were added and the reaction stirred for 2 days. The reaction mixture was diluted with EtOAc (25 mL) and then washed with water (10 mL), $NaHCO_3$ (10 mL), 1M HCl (10 mL) and brine (10 mL). The organic layer was dried with $MgSO_4$ and the solvent removed under reduced pressure. The crude residue was purified by flash column chromatography (PE/EtOAc on SiO_2) to yield the desired product as a white solid (56.7 mg, 0.124 mmol, 7%).

ν_{max} (film) cm^{-1} : 3252 (N-H), 2953 (C-H), 2927 (C-H), 2856 (C-H), 1591 (C=C), 1523 (C=C), 1493 (C=C), 1463 (C=C), 1337, 1282, 1260, 1150, 1092, 1061, 935, 902, 831, 812, 779, 747, 665, 562, 519, 460.

^1H NMR (400 MHz, $CDCl_3$) δ_H ppm: 8.75 (s, 1H), 8.18 (dd, J = 9.0, 2.6 Hz, 1H), 8.01 (d, J = 2.6 Hz, 1H), 7.69 (d, J = 9.1 Hz, 1H), 4.84 (s, 2H), 3.24 – 3.15 (m, 2H), 1.89 – 1.77 (m, 2H), 1.39 (q, J = 7.3 Hz, 2H), 1.31 – 1.19 (m, 8H), 0.94 (s, 9H), 0.86 (t, J = 7.0 Hz, 3H), 0.16 (s, 5H).

$^{13}C\{^1H\}$ NMR (101 MHz, $CDCl_3$) δ_C ppm: 144.0, 142.8, 128.0, 125.1, 124.0, 117.3, 65.3, 53.3, 31.8, 29.09, 29.0, 28.3, 25.8, 23.7, 22.7, 18.3, 14.2, -5.3.

HRMS: calc for $C_{21}H_{37}N_2O_5SSi^-$ $[M-H]^-$: 457.2192, found: 457.2201.

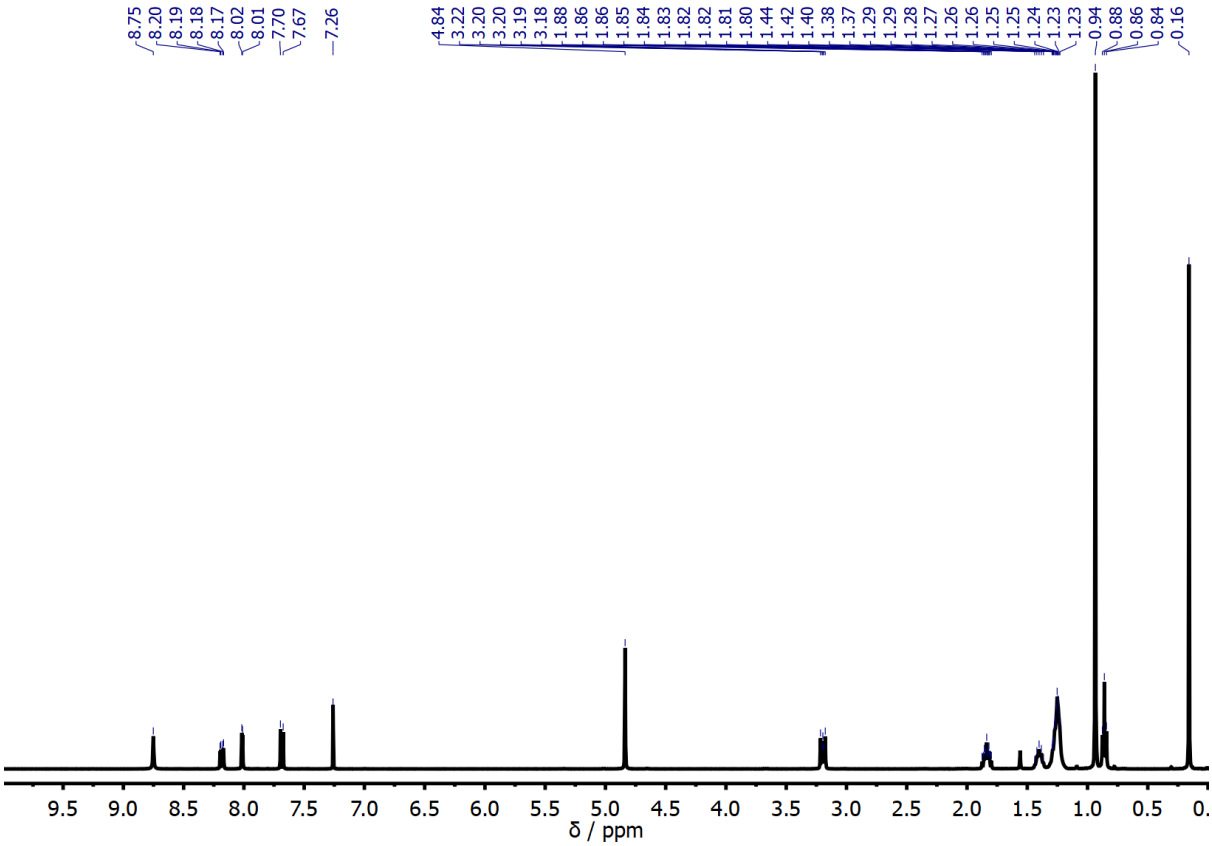

Figure S.4 – ^1H NMR spectrum of **2** in $CDCl_3$ (δ 0 – 12 ppm).

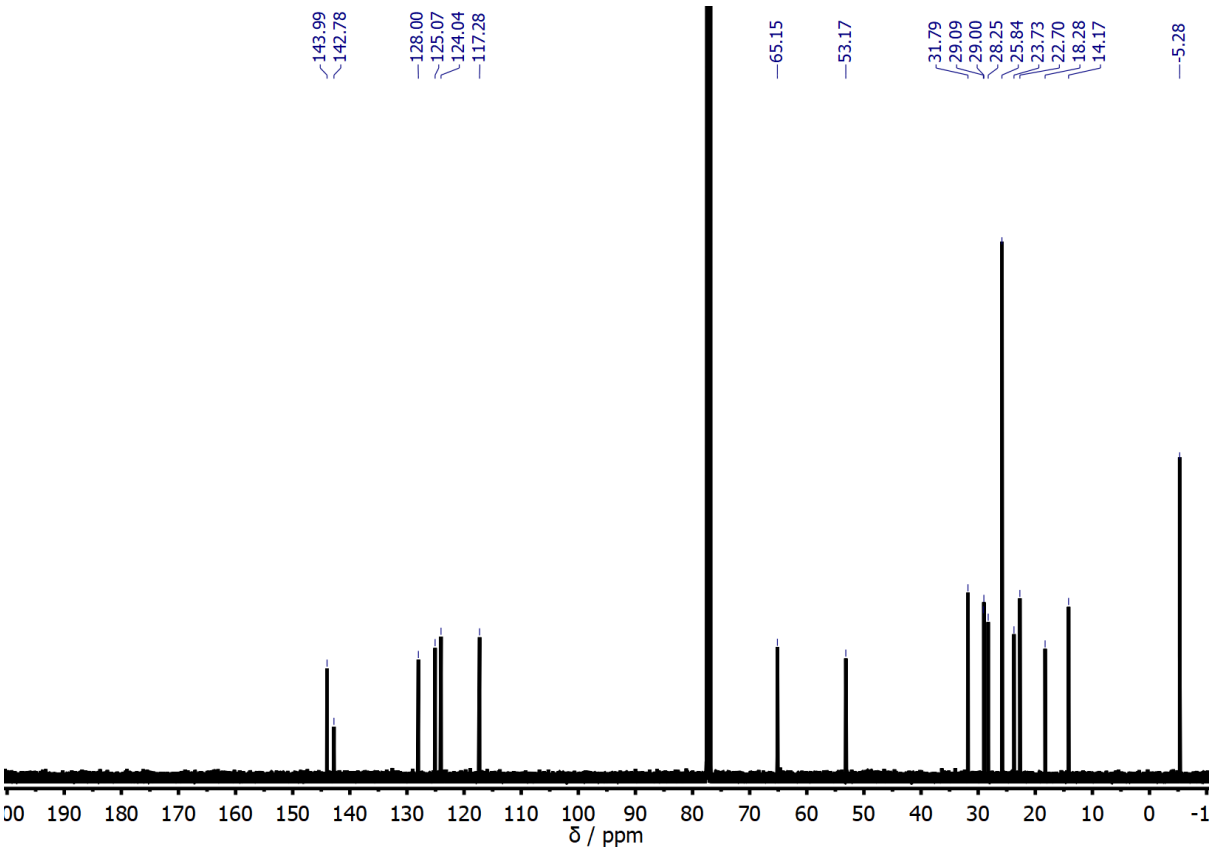

Figure S.5 – ^{13}C NMR spectrum of **2** in $CDCl_3$ (δ 0 – 200 ppm).

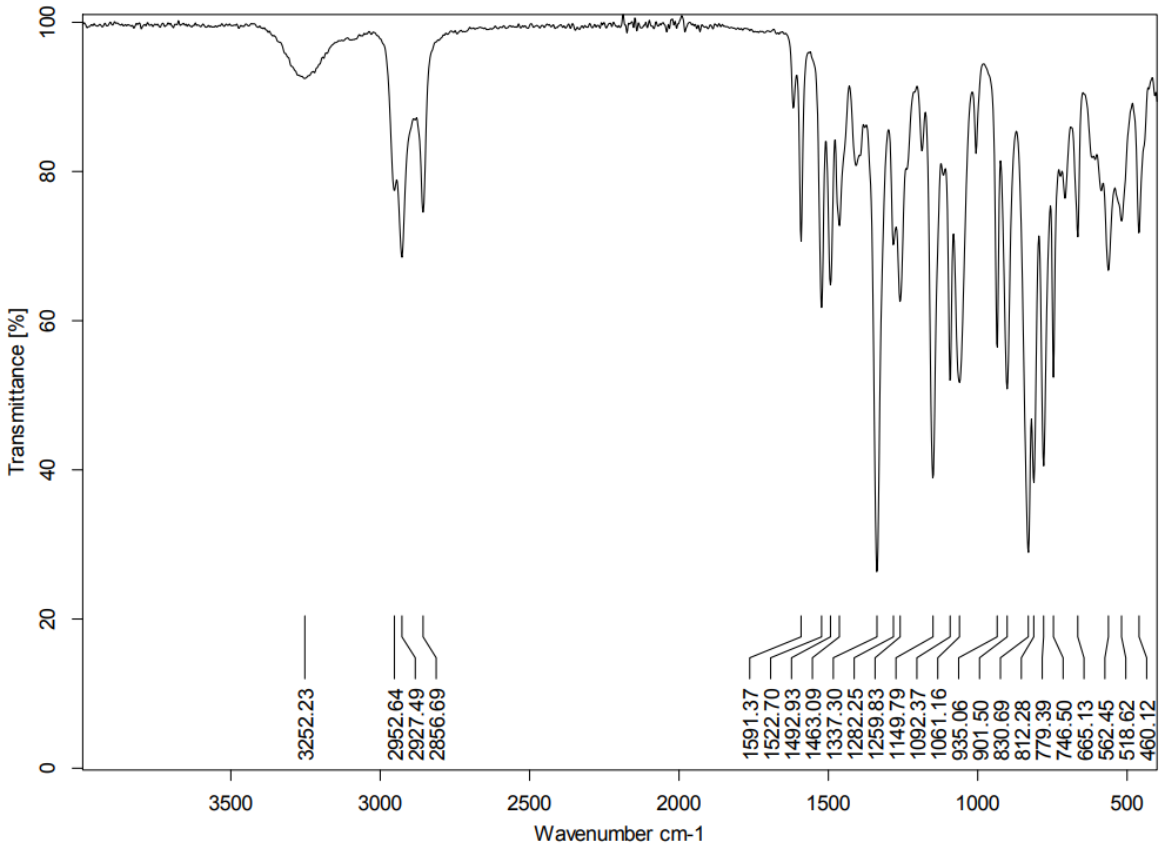

Figure S.6 – FT-IR spectrum of **2**.

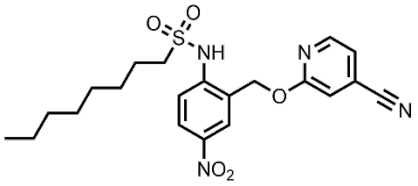

N-(2-(((4-cyanopyridin-2-yl)oxy)methyl)-4-nitrophenyl)octane-1-sulfonamide, **3**. N-(2-(((tert-butyldimethylsilyl)oxy)methyl)-4-nitrophenyl)octane-1-sulfonamide (43.5 mg, 0.0948 mmol) was dissolved in dry THF (1 mL) under N_2. TBAF (1 M in THF, 0.15 mL, 0.15 mmol) was added and the reaction stirred for one hour. The solvent was removed under reduced pressure and the residue partitioned between Et_2O (20 mL) and water (10 mL). The organic layer was then washed with saturated NH_4Cl solution (3 x 10 mL), dried with $MgSO_4$ and solvent removed under reduce pressure. The resulting residue was dissolved in dry DMF (0.5 mL) under N_2 and added to a solution of NaH (60% in mineral oil, 4.0 mg, 0.10 mmol) in dry DMF (0.5 mL). This was stirred for 15 minutes before a solution of 4-cyano-2-fluoropyridine (16.2, 0.132 mmol) in dry DMF (0.5 mL) was added. The reaction mixture was stirred overnight and diluted with EtOAc (25 mL), washed with water (2 x 10 mL), 5% LiCl solution (10 mL) and brine (10 mL). The organic layer was dried using $MgSO_4$ and solvent removed under reduced pressure. The crude residue was purified using flash chromatography (PE/EtOAc on SiO_2) to yield the desired product as a white solid (7.2 mg, 0.016 mmol, 17%).

ν_{max} (film) cm^{-1} : 3285 (N-H), 3113, 2927 (C-H), 2856 (C-H), 1605 (C=C), 1592 (C=C), 1551 (C=C), 1526 (C=C), 1414, 1338, 1307, 1285, 1150, 1094, 1016.

^1H NMR (400 MHz, $CDCl_3$) δ_H ppm: 10.57 (s, 1H), 8.43 (d, J = 5.3 Hz, 1H), 8.40 (d, J = 2.7 Hz, 1H), 8.25 (dd, J = 9.1, 2.7 Hz, 1H), 7.75 (d, J = 9.1 Hz, 1H), 7.22 (dd, J = 5.4, 1.3 Hz, 1H), 7.10 (t, J = 1.0 Hz, 1H), 5.49 (s, 2H), 3.24 – 3.13 (m, 2H), 1.74 (tt, J = 7.9, 6.5 Hz, 2H), 1.42 – 1.31 (m, 3H), 1.24 (d, J = 15.6 Hz, 9H), 0.86 (t, J = 6.7 Hz, 4H).

$^{13}C\{^1H\}$ NMR (101 MHz, $CDCl_3$) δ_C ppm: 162.9, 147.8, 143.5, 143.2, 129.2, 126.5, 124.8, 124.4, 119.3, 118.1, 115.8, 115.3, 65.6, 53.1, 31.8, 29.1, 29.0, 28.2, 23.6, 22.7, 14.2.

HRMS: calc for $C_{21}H_{25}N_4O_5S^-$ $[M-H]^-$: 445.1546, found: 455.1550.

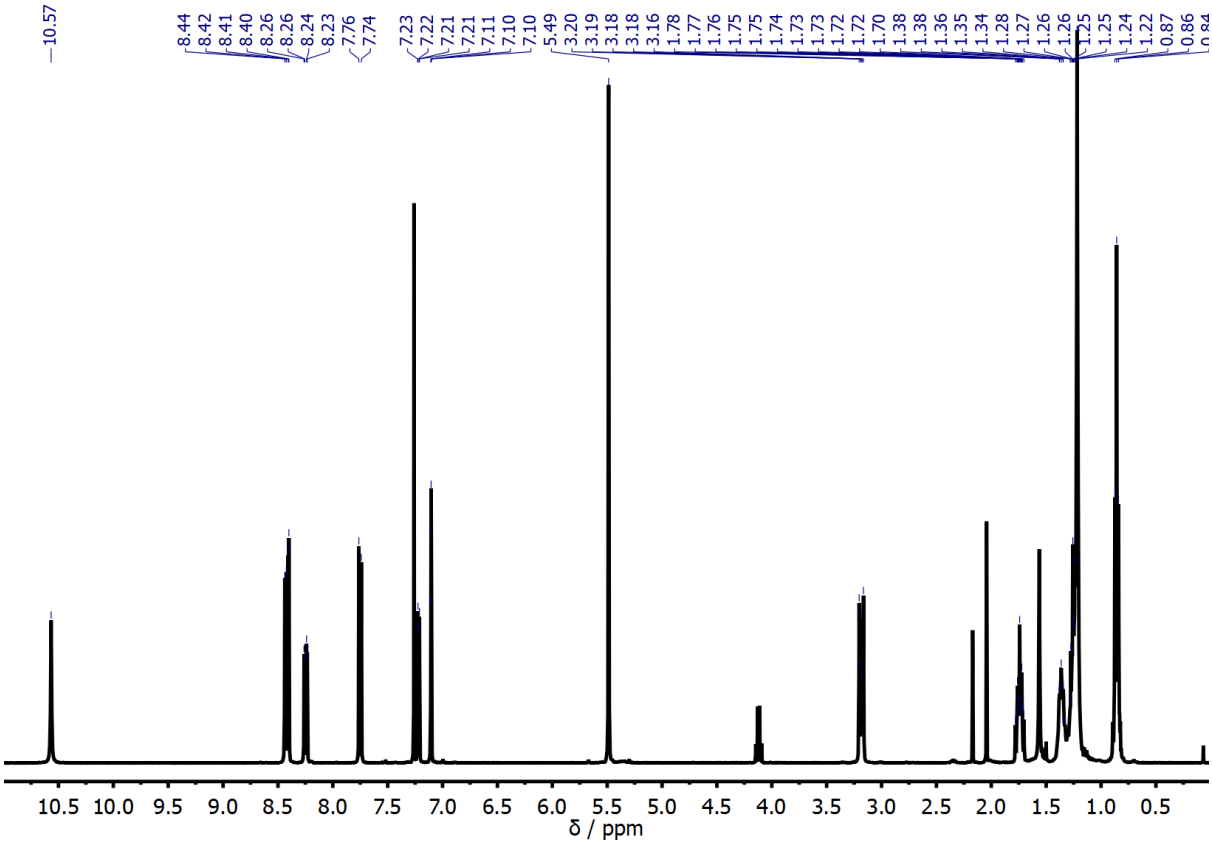

Figure S.7 – ^{1}H NMR spectrum of **3** in $CDCl_3$ (δ 0 – 12 ppm).

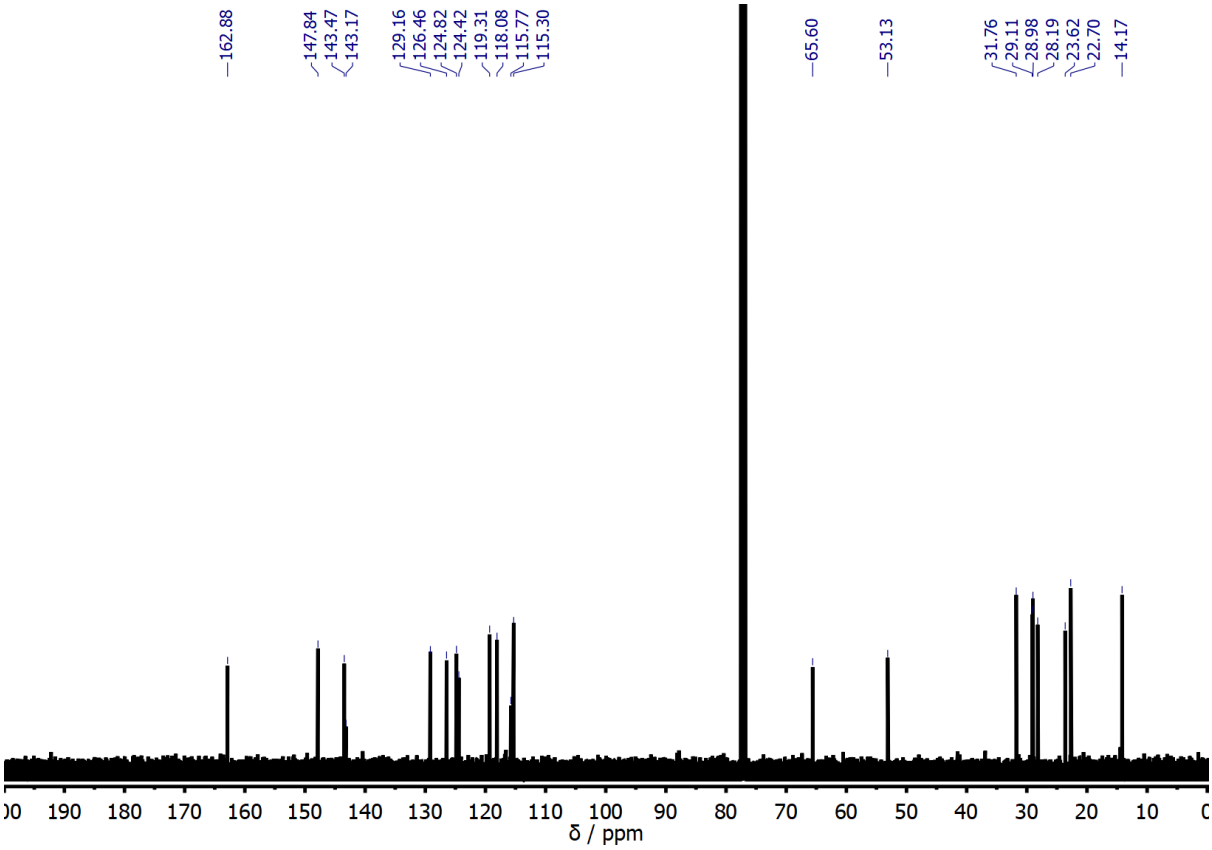

Figure S.8 – ^{13}C NMR spectrum of **3** in $CDCl_3$ (δ 0 – 200 ppm).

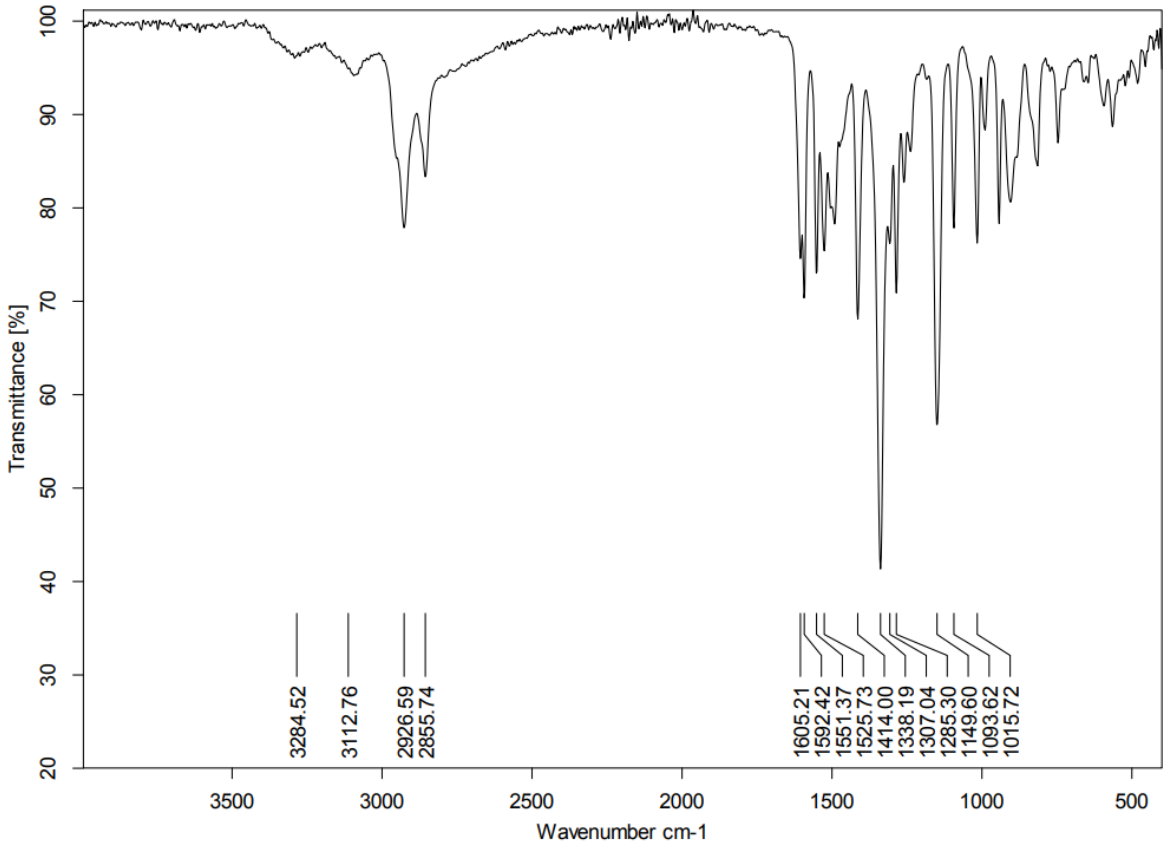

Figure S.9 – FT-IR spectrum of **3**.

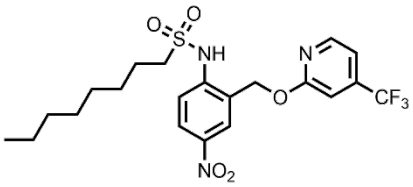

N-(4-nitro-2-(((4-(trifluoromethyl)pyridin-2-yl)oxy)methyl)phenyl)octane-1-sulfonamide, **4**. 4-nitro-2-(((4-(trifluoromethyl)pyridin-2-yl)oxy)methyl)aniline (18.5 mg, 0.0591 mmol) was dissolved in dry DCM (0.35 mL) under N_2. Pyridine (0.01 mL, 0.1 mmol) and 1-octane sulfonyl chloride (0.02 mL, 0.1 mmol) were added and the reaction stirred for 24 hours. The reaction mixture was diluted with EtOAc (25 mL) and then washed with water (10 mL), $NaHCO_3$ (10 mL), 1M HCl (10 mL) and brine (10 mL). The organic layer was dried with $MgSO_4$ and the solvent removed under reduced pressure. The crude residue was purified by flash column chromatography (PE/EtOAc on SiO_2) to yield the desired product as a white solid (0.75 mg, 0.0015 mmol, 3%).

ν_{max} (film) cm^{-1} : 2952 (C-H), 2925 (C-H), 2853 (C-C), 1592 (C=C), 1528 (C=C), 1421, 1336, 1176, 1146, 1008.

^1H NMR (400 MHz, $CDCl_3$) δ_H ppm: 10.93 (s, 1H), 8.44 (d, J = 5.5 Hz, 1H), 8.41 (d, J = 2.7 Hz, 1H), 8.25 (dd, J = 9.1, 2.6 Hz, 1H), 7.76 (d, J = 9.1 Hz, 1H), 7.22 (d, J = 5.3, 1H), 7.08 (s, 1H), 5.50 (s, 2H), 3.20 – 3.15 (m, 2H), 1.71 (q, J = 7.9 Hz, 2H), 1.63 (q, J = 7.6 Hz, 2H), 1.39 – 1.27 (m, 8H), 0.88 (t, J = 7.1 Hz, 3H).

$^{13}C\{^1H\}$ NMR (101 MHz, $CDCl_3$) δ_C ppm: 13C NMR (176 MHz, CDCl3) δ 163.2, 147.7, 129.2, 126.4, 118.0, 114.0, 65.6, 53.1, 31.8, 29.9, 29.8, 29.5, 29.1, 29.0, 23.6, 22.7, 14.2.

HRMS: calc for $C_{21}H_{25}F_3N_3O_5S^-$ $[M-H]^-$: 488.1467, found: 488.1474.

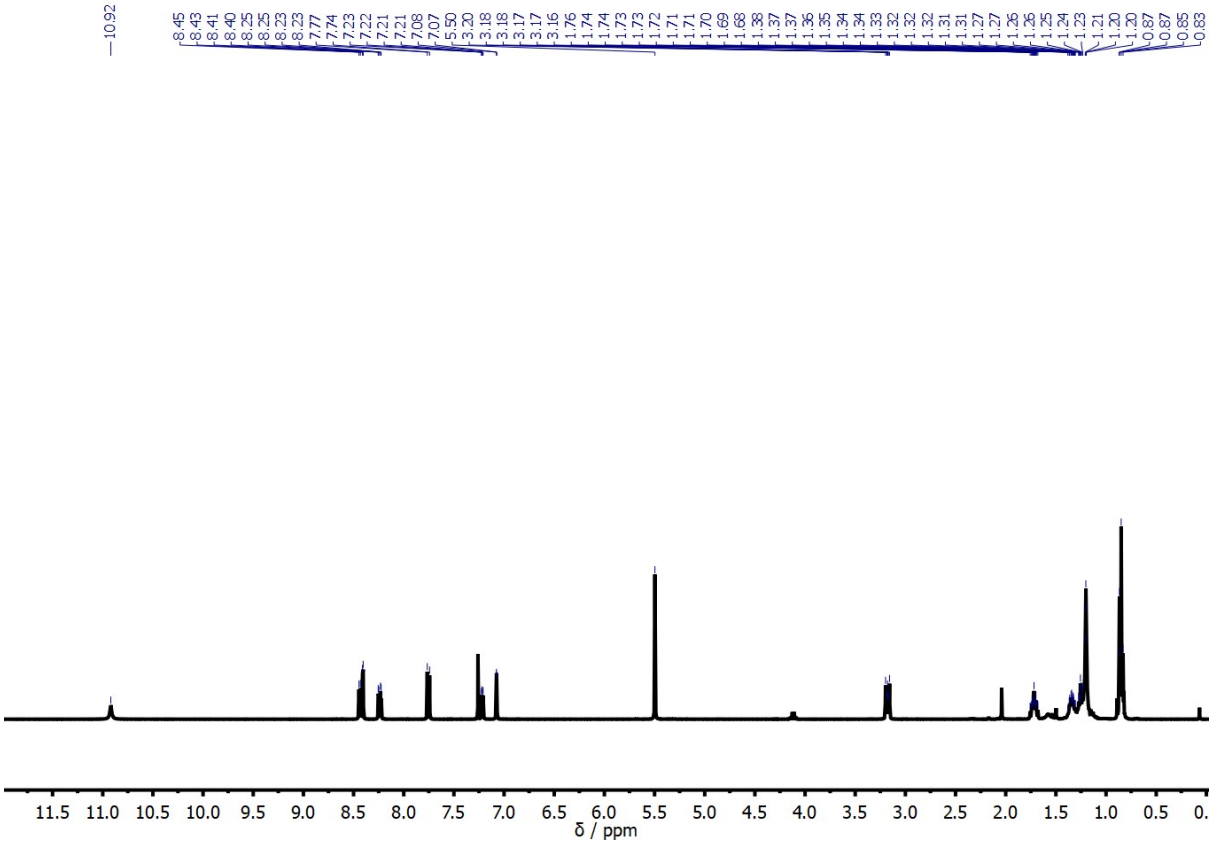

Figure S.10 – ^1H NMR spectrum of **4** in $CDCl_3$ (δ 0 – 12 ppm).

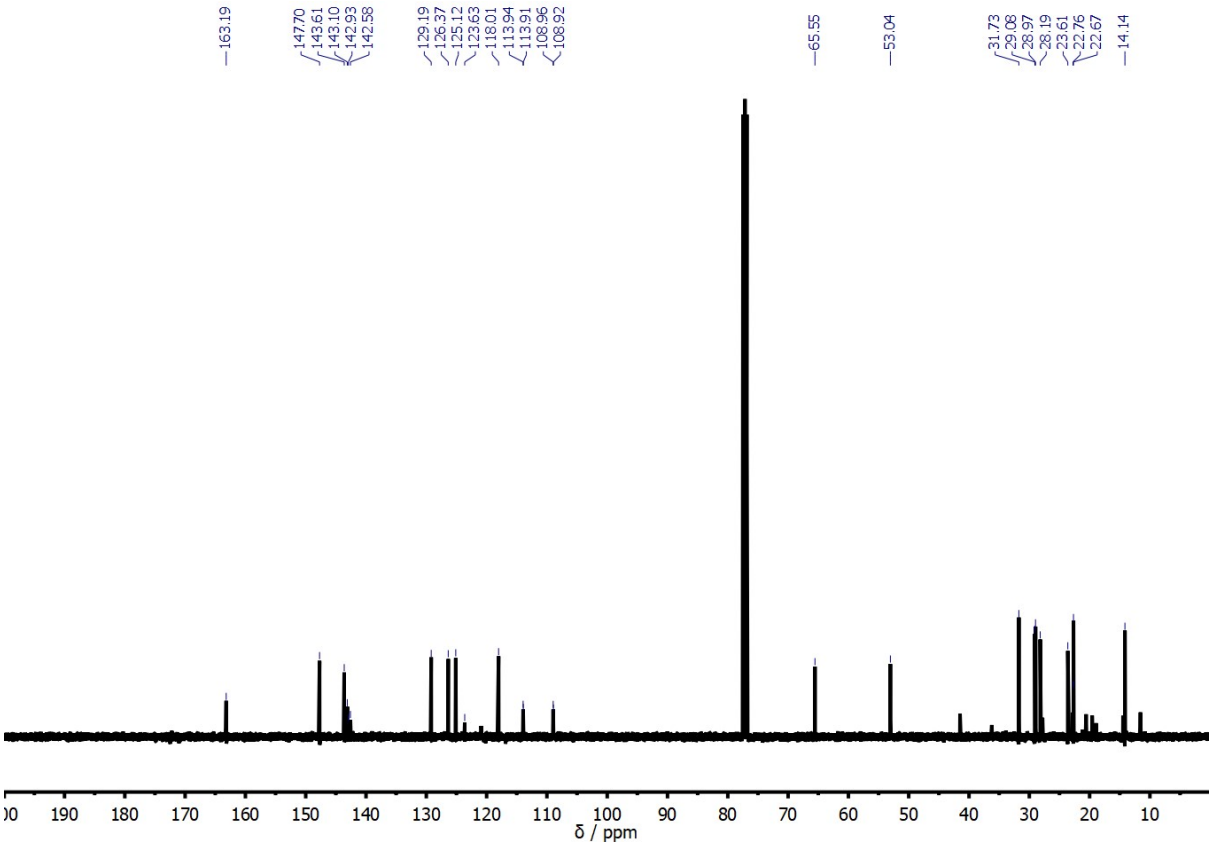

Figure S.11 – ^{13}C NMR spectrum of **4** in $CDCl_3$ (δ 0 – 200 ppm).

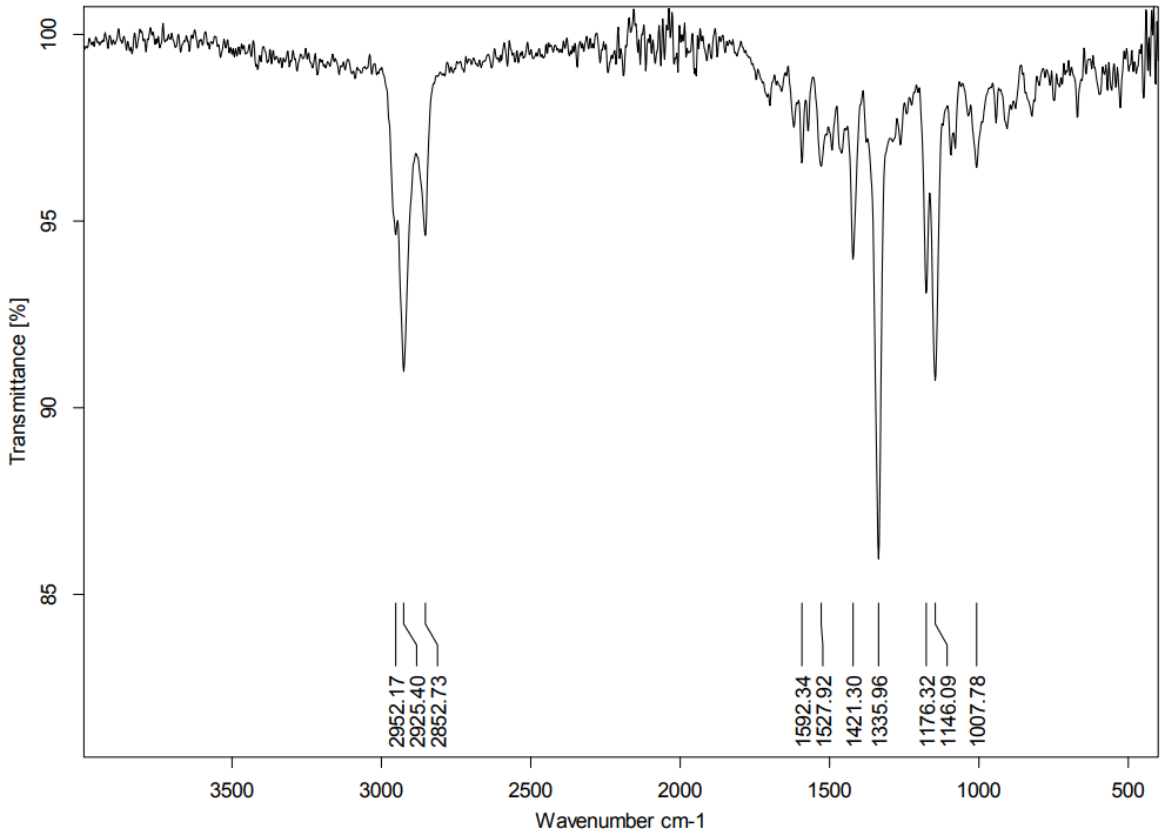

Figure S.12 – FT-IR spectrum of **4**.

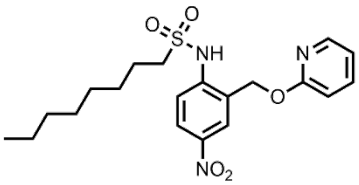

N-(4-nitro-2-((pyridin-2-yloxy)methyl)phenyl)octane-1-sulfonamide, **5**. 4-nitro-2-((pyridin-2-yloxy)methyl)aniline (41.8 mg, 0.170 mmol) was dissolved in dry DCM (5 mL) under a nitrogen atmosphere. Pyridine (0.02 mL, 0.25 mmol) and 1-octanesulfonyl chloride (0.05 mL, 0.22 mmol) were added and the reaction stirred overnight. The reaction mixture was diluted with EtOAc (25 mL) and washed with H_2O (10 mL), HCl (1 M, 10 mL) and brine (10 mL). The organic layer was dried with $MgSO_4$, and the solvent removed under reduced pressure. The crude residue was purified using flash chromatography (PE/EtOAc on SiO_2) to yield the desired product as a white amorphous solid (11.5 mg, 0.279 mmol, 16%)

ν_{max} (film) cm^{-1}: 2959 (C-H), 2927 (C-H), 2856 (C-H), 1592 (C=C), 1508 (C=C), 1434 (C=C), 1339, 1277, 1148, 1093, 907, 522.

^1H NMR (400 MHz, $CDCl_3$) δ_H ppm: 11.97 (s, 1H), 8.40 (d, J = 2.7 Hz, 1H), 8.28 (ddd, J = 5.3, 2.0, 0.8 Hz, 1H), 8.23 (dd, J = 9.1, 2.7 Hz, 1H), 7.75 (d, J = 9.1 Hz, 1H), 7.68 (ddd, J = 8.9, 7.2, 2.0 Hz, 1H), 7.01 (ddd, J = 7.1, 5.2, 0.9 Hz, 1H), 6.84 (dt, J = 8.3, 0.9 Hz, 1H), 5.43 (s, 2H), 3.30 – 2.96 (m, 2H), 1.76 – 1.66 (m, 2H), 1.30 – 1.16 (m, 8H), 0.85 (t, J = 7.0 Hz, 3H).

$^{13}C\{^1H\}$ NMR (101 MHz, $CDCl_3$) δ_C ppm: 161.4, 146.0, 143.9, 142.9, 140.8, 129.3, 126.2, 125.9, 118.2, 117.9, 112.2, 65.2, 52.9, 31.8, 29.1, 28.2, 22.7, 14.2.

HRMS: calc for $C_{20}H_{26}N_3O_5S^-$ $[M-H]^-$: 420.1593, found: 420.1594

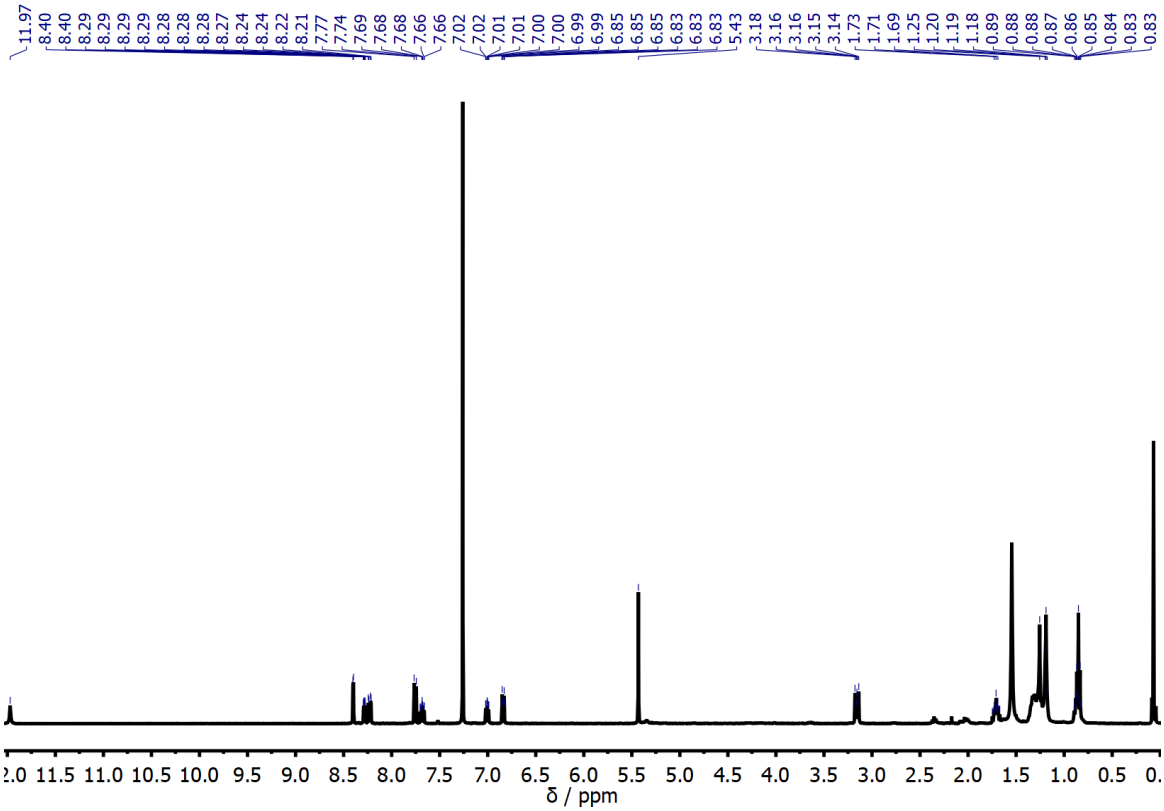

Figure S.13 – ^1H NMR spectrum of **5** in $CDCl_3$ (δ 0 – 12 ppm).

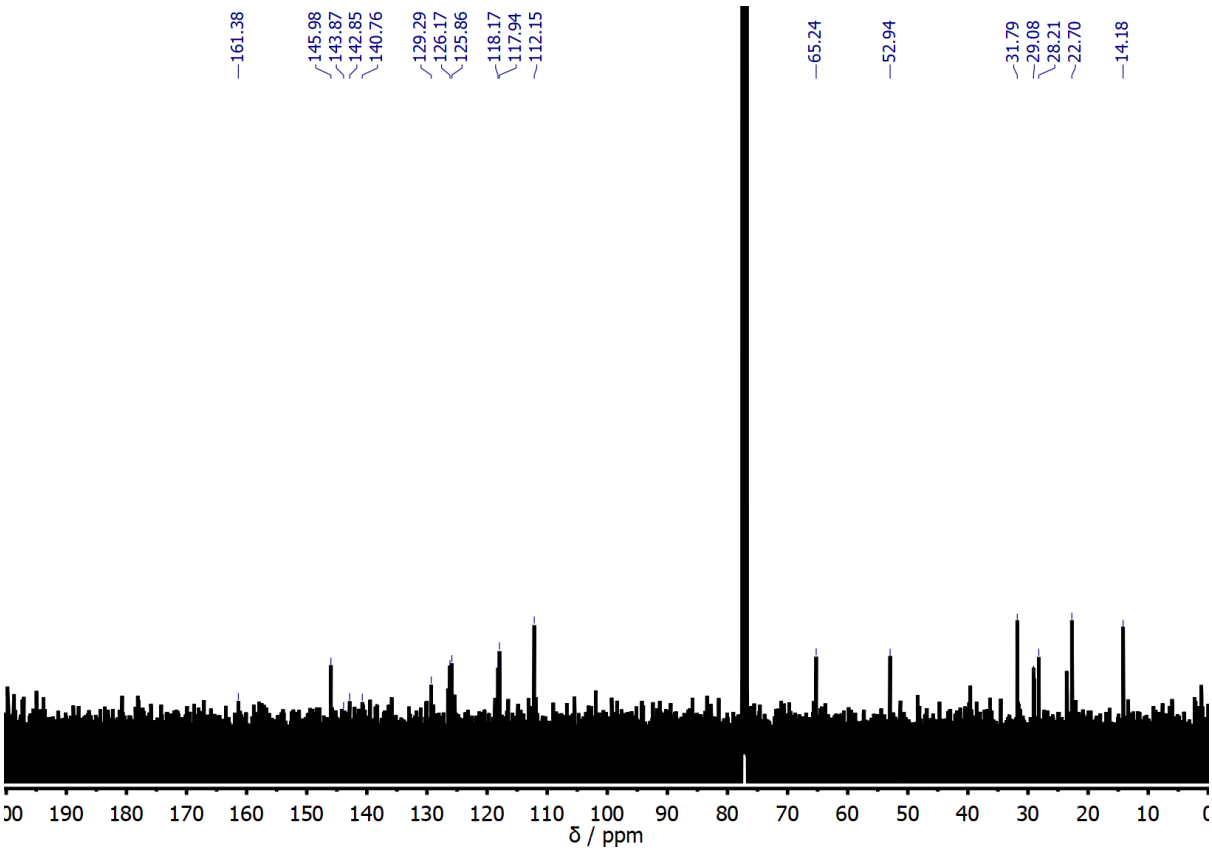

Figure S.14 – ^{13}C NMR spectrum of **5** in $CDCl_3$ (δ 0 – 200 ppm).

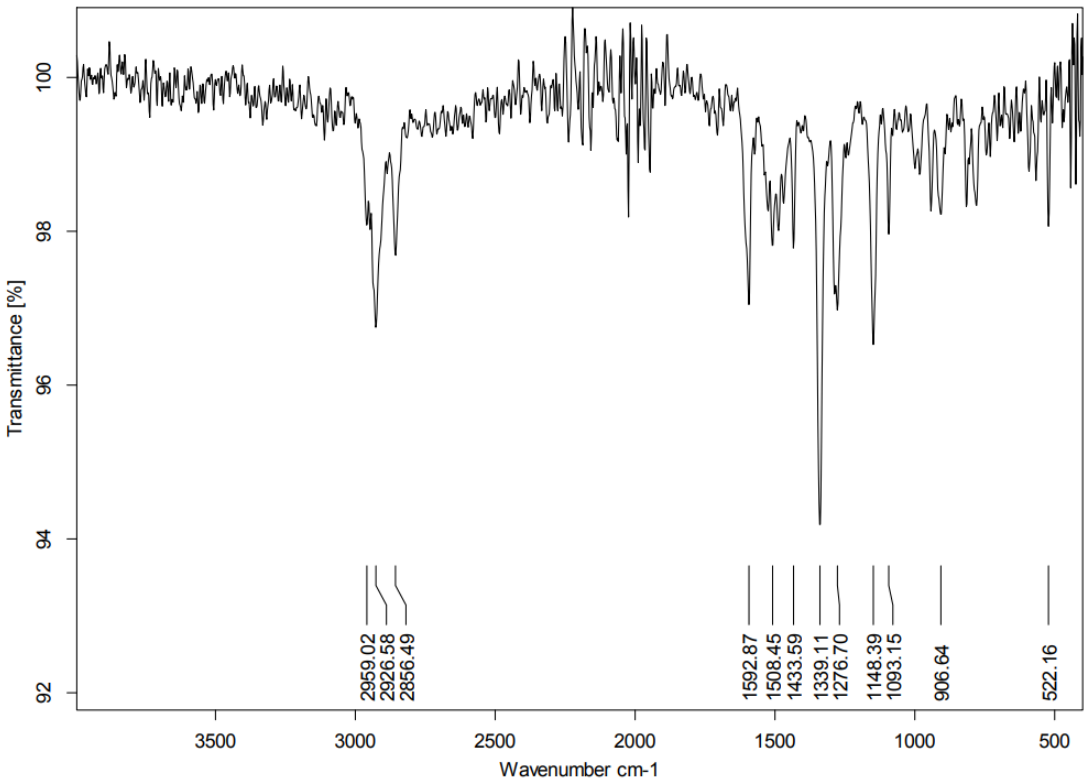

Figure S.15 – FT-IR spectrum of **5**.

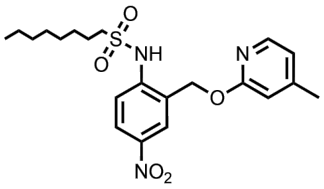

N-(2-(((4-methylpyridin-2-yl)oxy)methyl)-4-nitrophenyl)octane-1-sulfonamide, **6**. 4-nitro-2-((4-methylpyridin-2-yloxy)methyl)aniline (20.1 mg, 0.0775 mmol) was dissolved in dry DCM (1 mL) under a nitrogen atmosphere. Pyridine (0.05 mL, 0.62 mmol) and 1-octanesulfonyl chloride (0.20 mL, 0.86 mmol) were added and the reaction stirred for a day. The reaction mixture was diluted with EtOAc (25 mL) and washed with H_2O (10 mL), HCl (1 M, 10 mL), saturated $NaHCO_3$ (10 mL) and brine (10 mL). The organic layer was dried with $MgSO_4$, and the solvent removed under reduced pressure. The crude residue was purified using flash chromatography (PE/EtOAc on SiO_2) to yield the desired product as a white amorphous solid (1.78 mg, 0.00409 mmol, 5%)

ν_{max} (film) cm^{-1} : 2955 (C-H), 2924 (C-H), 2854 (C-H), 1615 (C=C), 1593 (C=C), 1510 (C=C), 1489 (C=C), 1338, 1310, 1286, 1262, 1149, 1093.

^1H NMR (400 MHz, $CDCl_3$) δ_H ppm: 12.24 (s, 1H), 8.39 (d, J = 2.7 Hz, 1H), 8.22 (dd, J = 9.1, 2.7 Hz, 1H), 8.13 (dd, J = 5.4, 0.7 Hz, 1H), 7.75 (d, J = 9.1 Hz, 1H), 6.82 (ddd, J = 5.4, 1.4, 0.7 Hz, 1H), 6.64 (dt, J = 1.5, 0.8 Hz, 1H), 5.40 (s, 2H), 3.18 – 3.11 (m, 2H), 2.33 (t, J = 0.7 Hz, 3H), 1.73 – 1.67 (m, 2H), 1.32 (t, J = 7.2 Hz, 2H), 1.28-1.22 (m, 2H), 1.20-1.17 (m, 6H), 0.85 (t, J = 7.2 Hz, 3H).

$^{13}C\{^1H\}$ NMR (101 MHz, $CDCl_3$) δ_C ppm: 162.3, 152.5, 145.3, 144.2, 142.9, 129.3, 126.1, 119.7, 117.9, 112.0, 65.2, 52.9, 31.8, 29.1, 29.0, 28.2, 23.6, 22.7, 21.3, 14.2.

HRMS: calc for $C_{21}H_{30}N_3O_5S^+$ $[M+H]^+$: 436.1906, found: 436.1895.

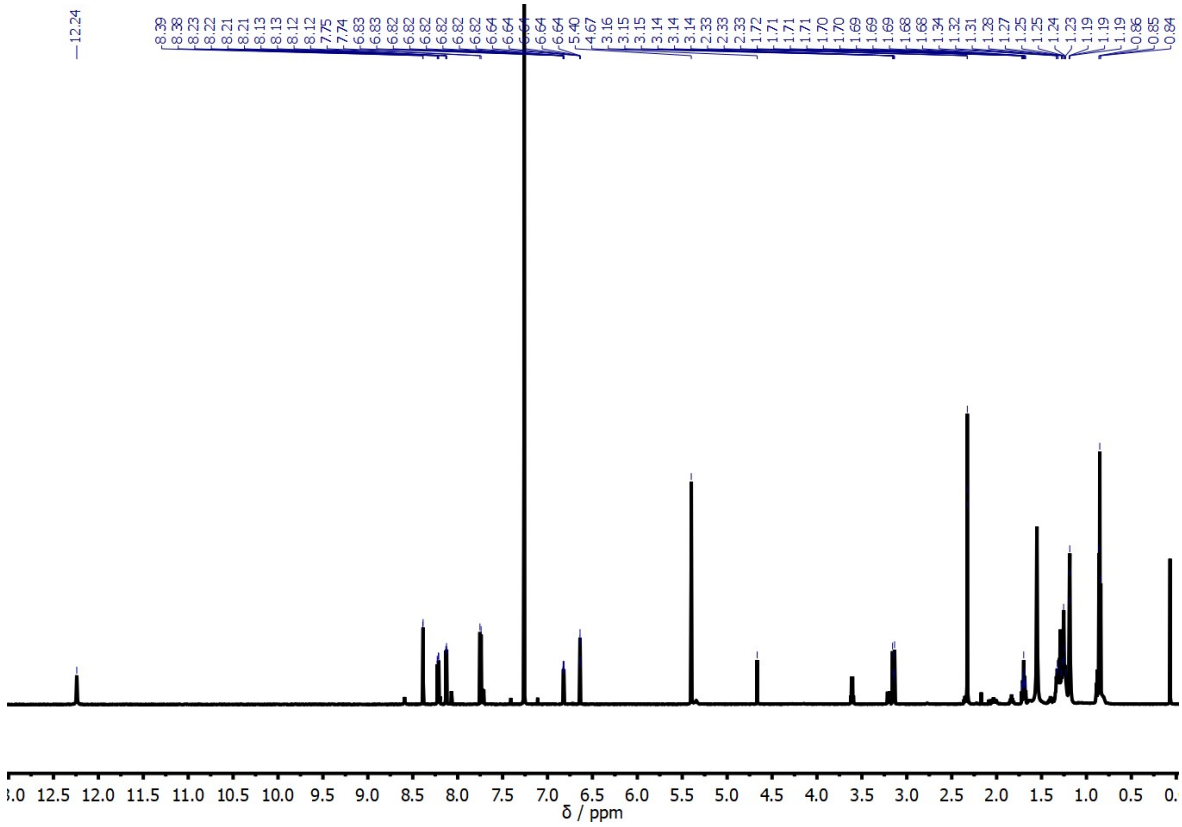

Figure S.16 – ^1H NMR spectrum of **6** in $CDCl_3$ (δ 0 – 13 ppm).

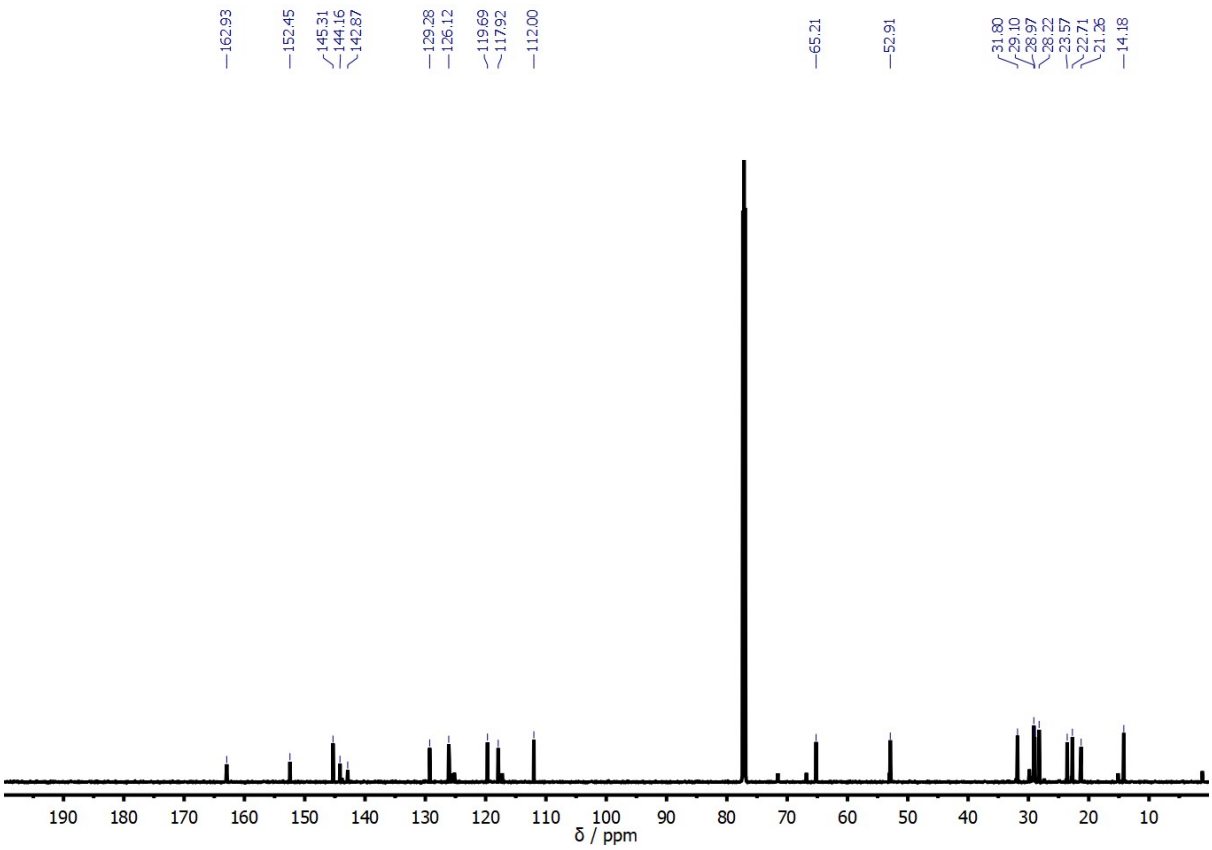

Figure S.17 – ^{13}C NMR spectrum of **6** in $CDCl_3$ (δ 0 – 200 ppm).

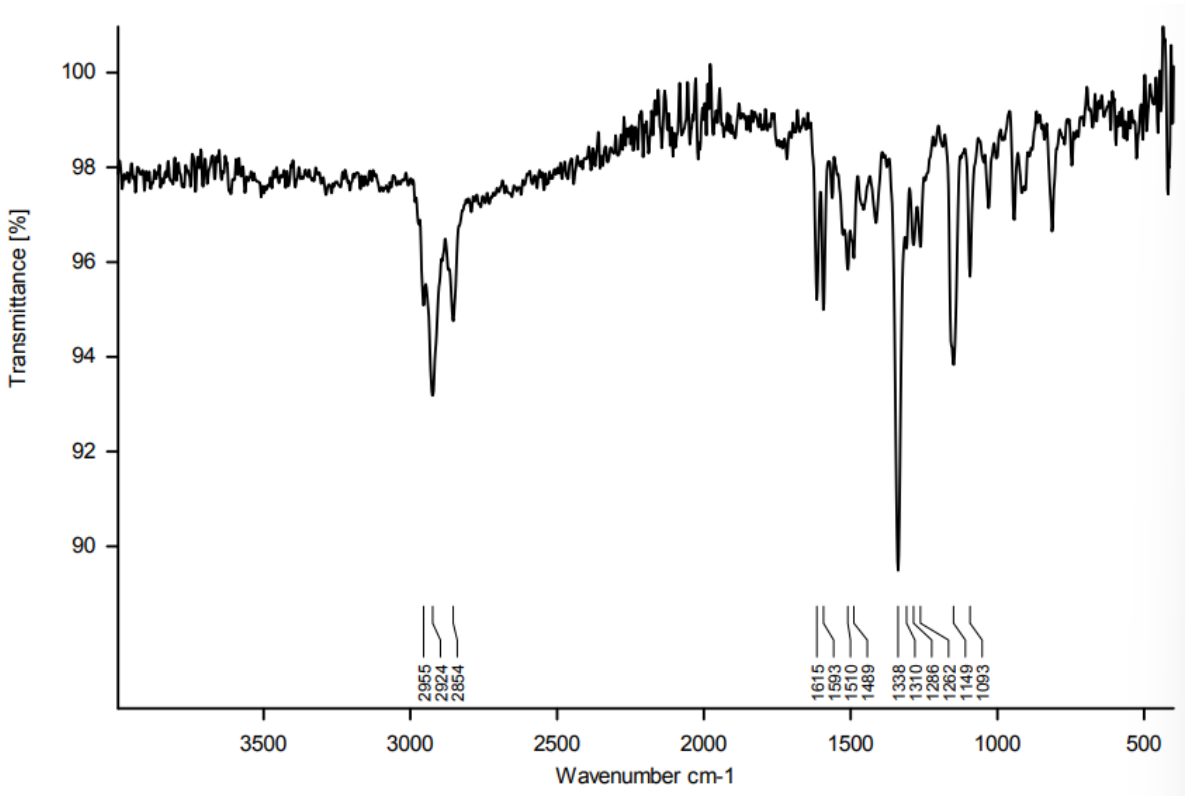

Figure S.18 – FT-IR spectrum of **6**.

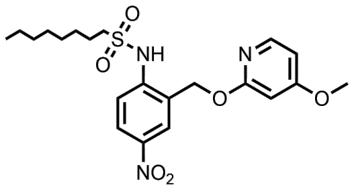

N-(2-(((4-methoxypyridin-2-yl)oxy)methyl)-4-nitrophenyl)octane-1-sulfonamide, **7**. 4-nitro-2-((4-methoxypyridin-2-yloxy)methyl)aniline (34.1 mg, 0.124 mmol) was dissolved in dry DCM (1 mL) under a nitrogen atmosphere. Pyridine (0.05 mL, 0.62 mmol) and 1-octanesulfonyl chloride (0.20 mL, 0.86 mmol) were added and the reaction stirred for a day. The reaction mixture was diluted with EtOAc (25 mL) and washed with H_2O (10 mL), HCl (1 M, 10 mL), saturated $NaHCO_3$ (10 mL) and brine (10 mL). The organic layer was dried with $MgSO_4$, and the solvent removed under reduced pressure. The crude residue was purified using flash chromatography (PE/EtOAc on SiO_2) to yield the desired product as a white amorphous solid (0.91 mg, 0.00202 mmol, 2%)

ν_{max} (film) cm^{-1} : 2956 (C-H), 2924 (C-H), 2854 (C-H), 1609 (C=C), 1594 (C=C), 1573 (C=C), 1508 (C=C), 1489 (C=C), 133, 1244, 1202, 1164, 1148, 1093, 1038.

^1H NMR (400 MHz, $CDCl_3$) δ_H ppm: 12.44 (s, 1H), 8.38 (d, J = 2.7 Hz, 1H), 8.22 (dd, J = 9.1, 2.7 Hz, 1H), 8.08 (d, J = 6.1 Hz, 1H), 7.75 (d, J = 9.1 Hz, 1H), 6.57 (dd, J = 6.1, 2.2 Hz, 1H), 6.26 (d, J = 2.2 Hz, 1H), 5.40 (s, 2H), 3.83 (s, 3H), 3.26 – 3.05 (m, 2H), 1.73 – 1.67 (m, 2H), 1.36 – 1.30 (m, 2H), 1.27 – 1.24 (m, 2H), 1.21 – 1.18 (m, 6H), 0.85 (t, J = 7.2 Hz, 3H).

$^{13}C\{^1H\}$ NMR (101 MHz, $CDCl_3$) δ_C ppm: 169.2, 164.7, 146.4, 144.3, 142.8, 129.3, 126.2, 125.9, 117.9, 94.8, 55.7, 52.9, 29.1, 29.0, 28.2, 23.6, 22.7.

HRMS: calc for $C_{21}H_{30}N_3O_6S^+$ $[M+H]^+$: 452.1855, found: 452.1841.

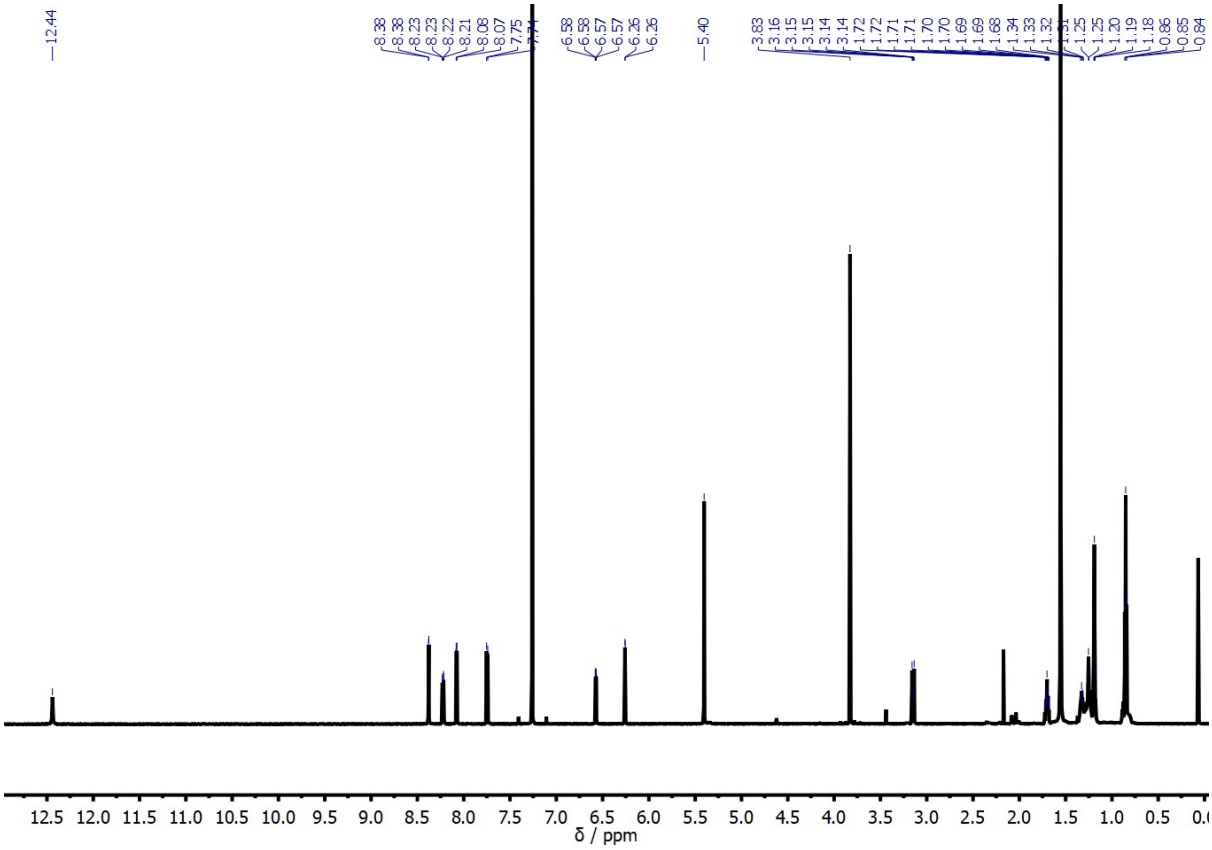

Figure S.19 – ^{1}H NMR spectrum of **7** in $CDCl_3$ (δ 0 – 13 ppm).

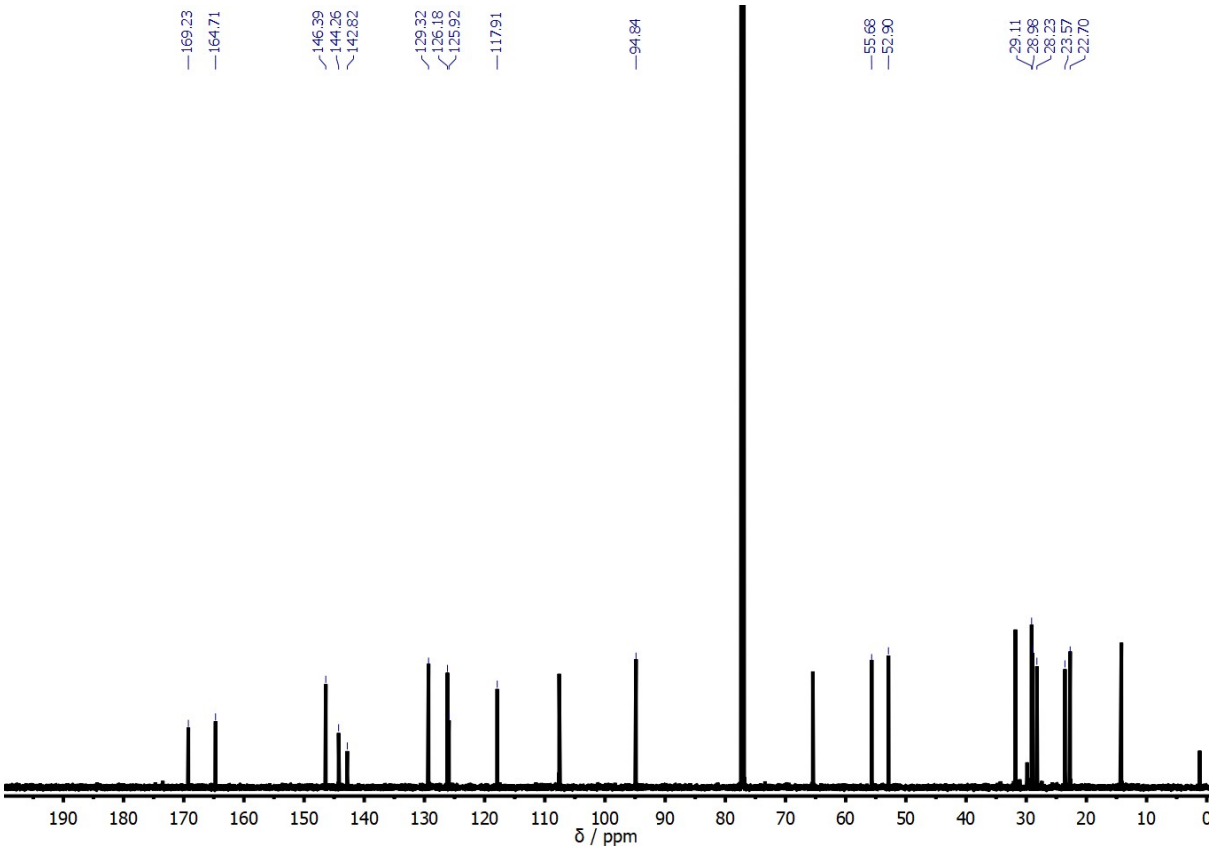

Figure S.20 – ^{13}C NMR spectrum of **7** in $CDCl_3$ (δ 0 – 200 ppm).

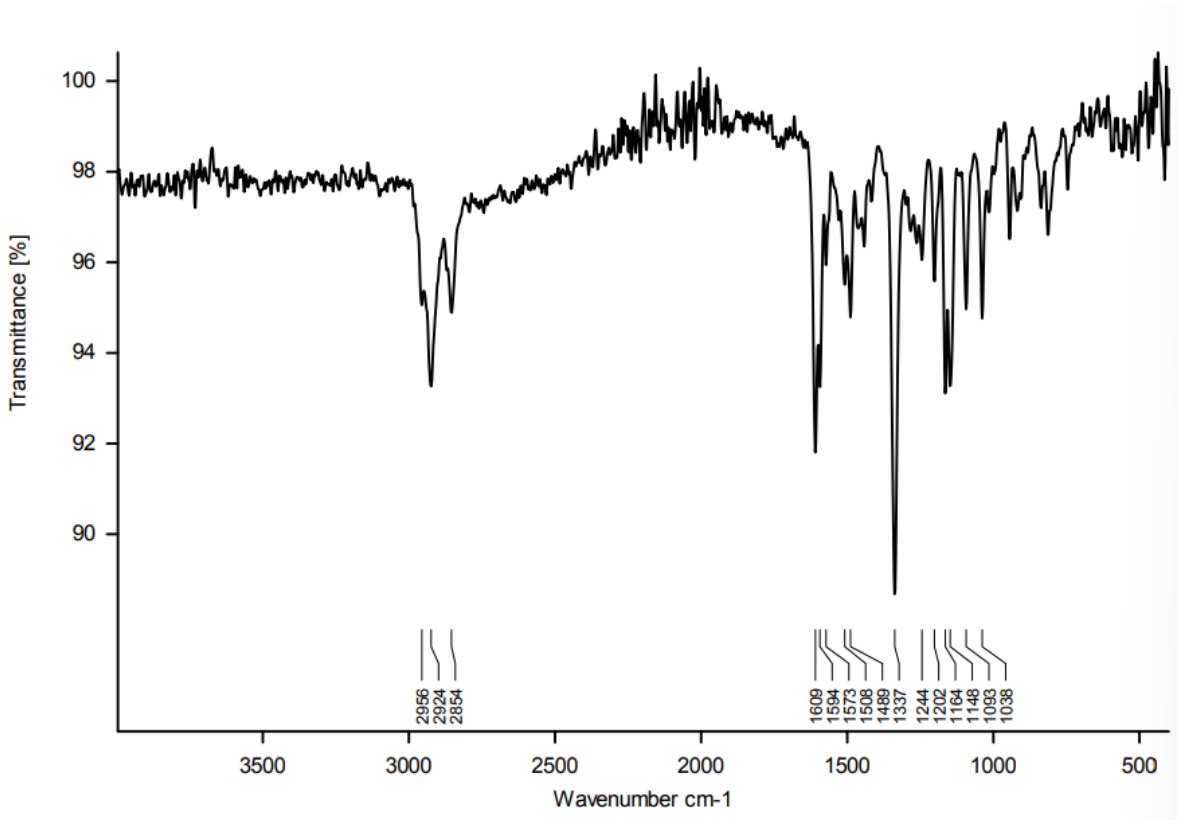

Figure S.21 – FT-IR spectrum of **7**.

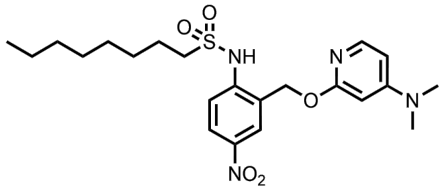

N-(2-(((4-dimethylaminopyridin-2-yl)oxy)methyl)-4-nitrophenyl)octane-1-sulfonamide, **8**. 4-nitro-2-((4-dimethylaminopyridin-2-yloxy)methyl)aniline (17.0 mg, 0.124 mmol) and sodium hydride (60% dispersion in mineral oil, 2.6 mg, 0.065 mmol) were dissolved in dry DMF (0.5 mL) under a nitrogen atmosphere. 1-octanesulfonyl chloride (0.02 mL, 0.086 mmol) was added and the reaction stirred for 15 minutes. The reaction mixture was diluted with EtOAc (25 mL) and washed with H_2O (10 mL), saturated $NaHCO_3$ (10 mL), 5% LiCL solution (10 mL) and brine (10 mL). The organic layer was dried with $MgSO_4$, and the solvent removed under reduced pressure. The crude residue was purified using flash chromatography (PE/EtOAc on SiO_2 then DCM/MeOH on Al_2O_3) to yield the desired product as a white solid (0.7 mg, 0.00166 mmol, 1%)

ν_{max} (film) cm^{-1} : 2949 (C-H), 2927 (C-H), 2852 (C-H), 1614 (C=C), 1593 (C=C), 1526 (C=C), 1509 (C=C). 1445, 1337, 1285, 1266, 1147, 1093, 1033, 814

^1H NMR (400 MHz, $CDCl_3$) δ_H ppm: 13.45 (s, 1H), 8.36 (d, J = 2.7 Hz, 1H), 8.21 (dd, J = 9.1, 2.7 Hz, 1H), 7.93 (d, J = 6.4 Hz, 1H), 7.74 (d, J = 9.1 Hz, 1H), 6.29 (dd, J = 6.4, 2.3 Hz, 1H), 5.89 (d, J = 2.3 Hz, 1H), 5.35 (s, 2H), 3.18 – 3.10 (m, 2H), 2.99 (s, 6H), 1.75 – 1.64 (m, 2H), 1.31 (p, J = 7.3 Hz, 2H), 1.28 – 1.22 (m, 2H), 1.20 – 1.17 (m, 6H), 0.85 (t, J = 7.2 Hz, 3H).

$^{13}C\{^1H\}$ NMR (101 MHz, $CDCl_3$) δ_C ppm: 164.0, 157.7, 145.2, 144.8, 142.6, 129.3, 126.4, 126.0, 117.8, 103.4, 91.0, 65.4, 52.8, 31.8, 29.0, 28.3, 23.6, 22.7, 14.2.

HRMS: calc for $C_{22}H_{33}N_4O_5S^+$ $[M+H]^+$: 465.2172, found: 465.2164.

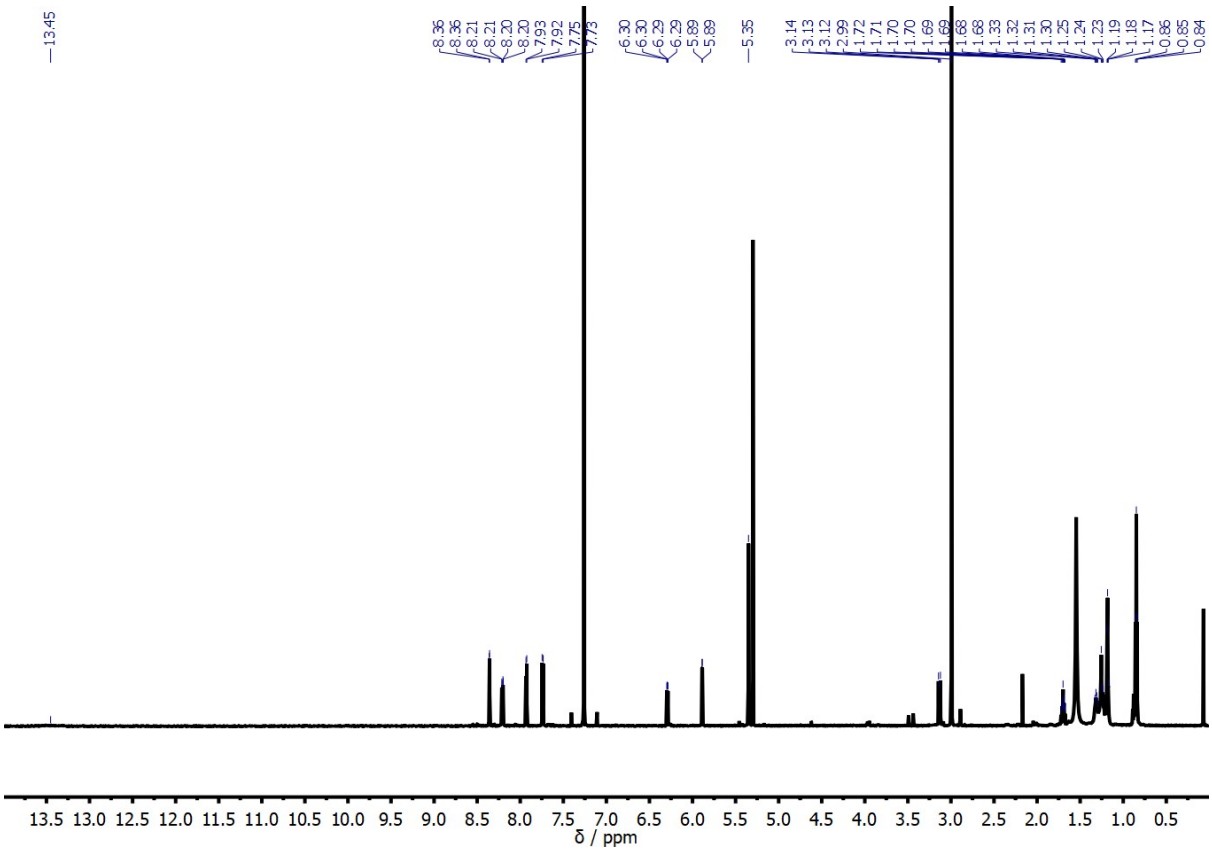

Figure S.22 – ^{1}H NMR spectrum of **8** in $CDCl_3$ (δ 0 – 14 ppm).

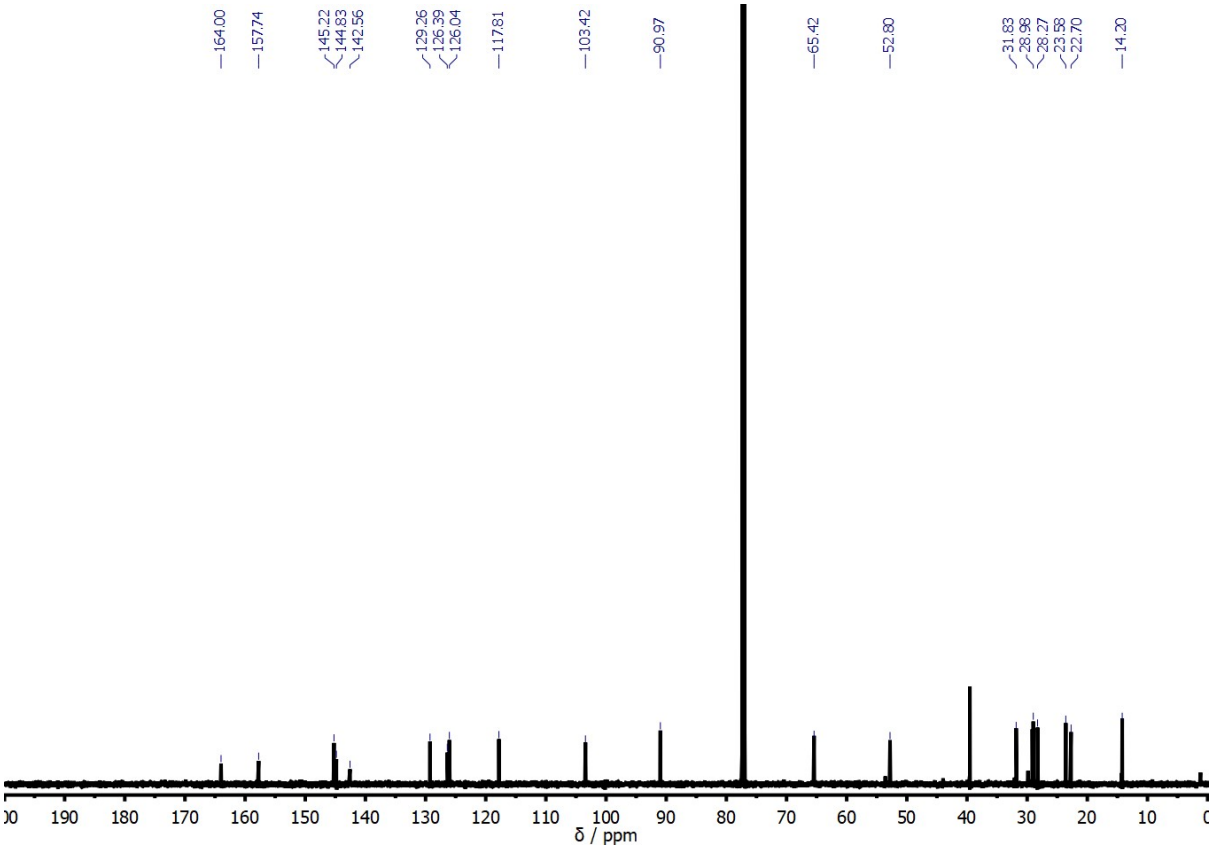

Figure S.23 – ^{13}C NMR spectrum of **8** in $CDCl_3$ (δ 0 – 200 ppm).

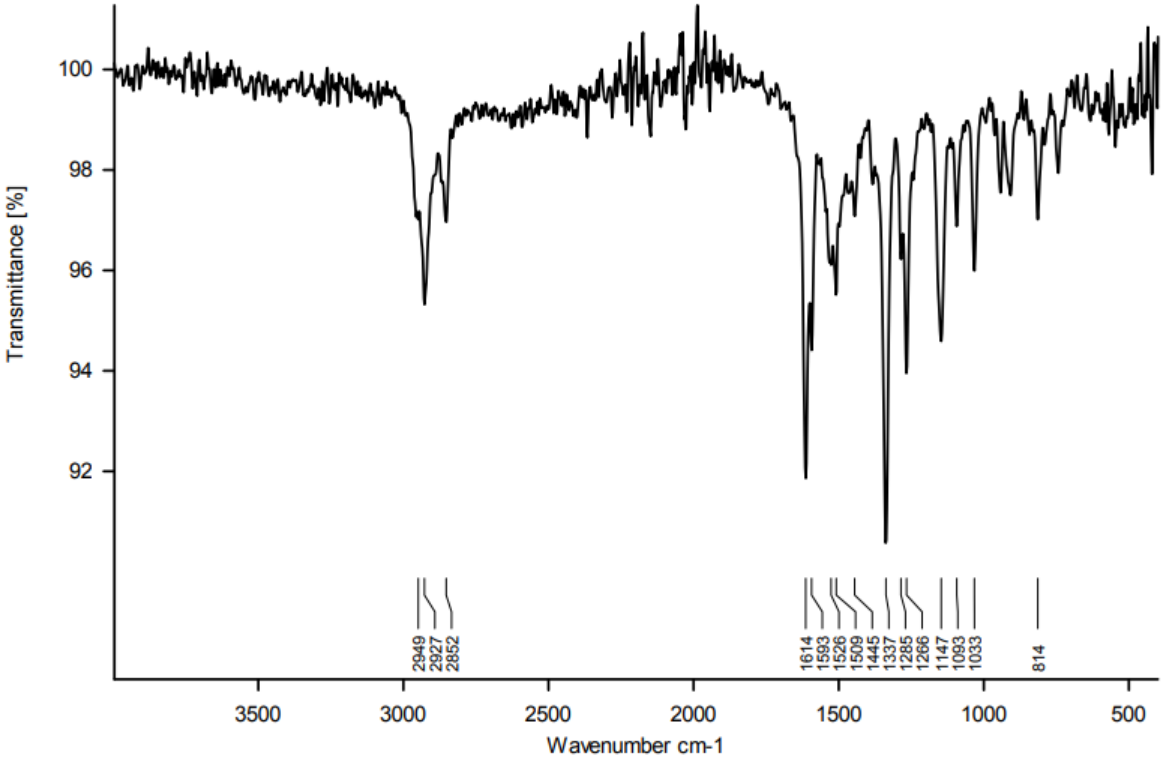

Figure S.24 – FT-IR spectrum of **8**.

UV-vis Absorption and ^{1}H NMR Titration Data

UV-vis titrations were carried out on an Agilent Cary 60 UV-Vis spectrophotometer, using standard titration protocols. A 5 mL sample of the host (**1-11**) was prepared at a known concentration (typically between 0.020-0.070 mM) in *n*-octane. The UV-vis spectrum of the free host (2 mL) was recorded. The guest (PFTB) was dissolved in 2 mL of the host solution to keep the concentration of host constant throughout the titration. Aliquots of the guest solution were successively added to the cuvette, and the UV-vis absorption spectrum was recorded after each addition. The UV-vis absorption spectra were analysed using a purpose-built Python script to fit the changes in the absorption at all wavelengths to a 1:2 binding isotherm. The quoted errors are worked out from twice the standard error of the mean from at least 3 repeats, to give values of the error at the 95% confidence interval.

NMR titrations were carried out on a Bruker 400 MHz spectrometer, using standard titration protocols and solvent suppression to deal with using *n*-octane as solvent. A capillary of DMSO-d_6 was inserted in the NMR tube alongside the titration solutions to act as a lock signal and the shift of the DMSO-d_6 signal was used to reference all spectra. A 2 mL sample of the host was prepared at a concentration of 0.18-0.22 mM in *n*-octane. The NMR spectrum of the host solution (0.6 mL) was recorded. The guest PFTB solution was prepared at a known concentration using the host solution as solvent to keep the concentration of the host constant throughout the titration. Aliquots of the guest solution were successively added to the NMR sample tube containing the host solution, and the ^{1}H NMR spectrum was recorded after each addition. The NMR spectra were analysed using a purpose-built Python script to fit the changes in the chemical shifts for different protons to a 1:2 binding isotherm.

For the NMR dilution experiment, 0.6 mL of a solution of the host at a known concentration in *n*-octane was placed in an NMR tube and aliquots of *n*-octane were added with the spectrum being recorded after every addition. A capillary of DMSO-d_6 was inserted in the NMR tube alongside the dilution solutions to act as a lock signal and the shift of the DMSO-d_6 signal was used to reference all spectra.

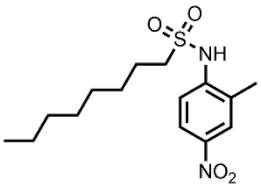

Figure S.25 – Structure of the host **1**.

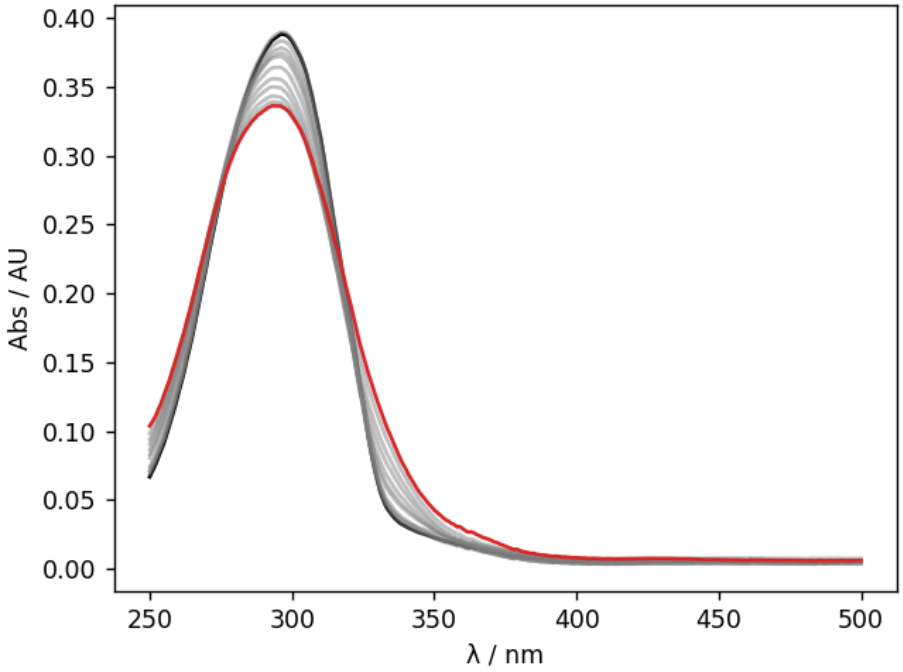

Figure S.26 - UV-vis absorption spectra for the titration of PFTB into **1** (0.0404 mM in *n*-octane, at 298K). The UV-vis spectrum of the host **1** and the final point of the titration are reported in black and in red, respectively.

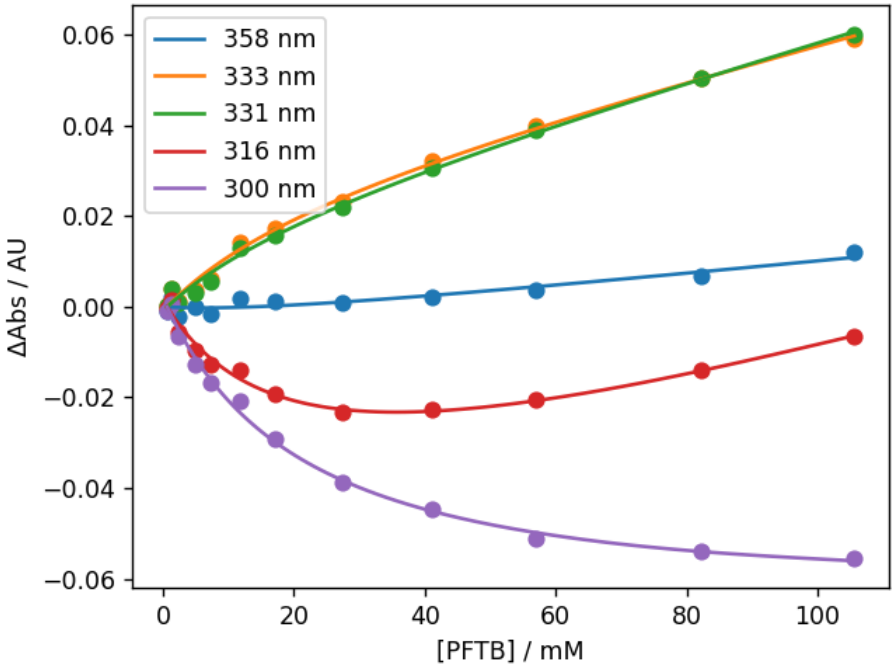

Figure S.27 - The fit of the absorbance at selected wavelengths to a 1:2 binding isotherm for the titration of PFTB into **1** (0.0404 mM in *n*-octane, at 298 K).

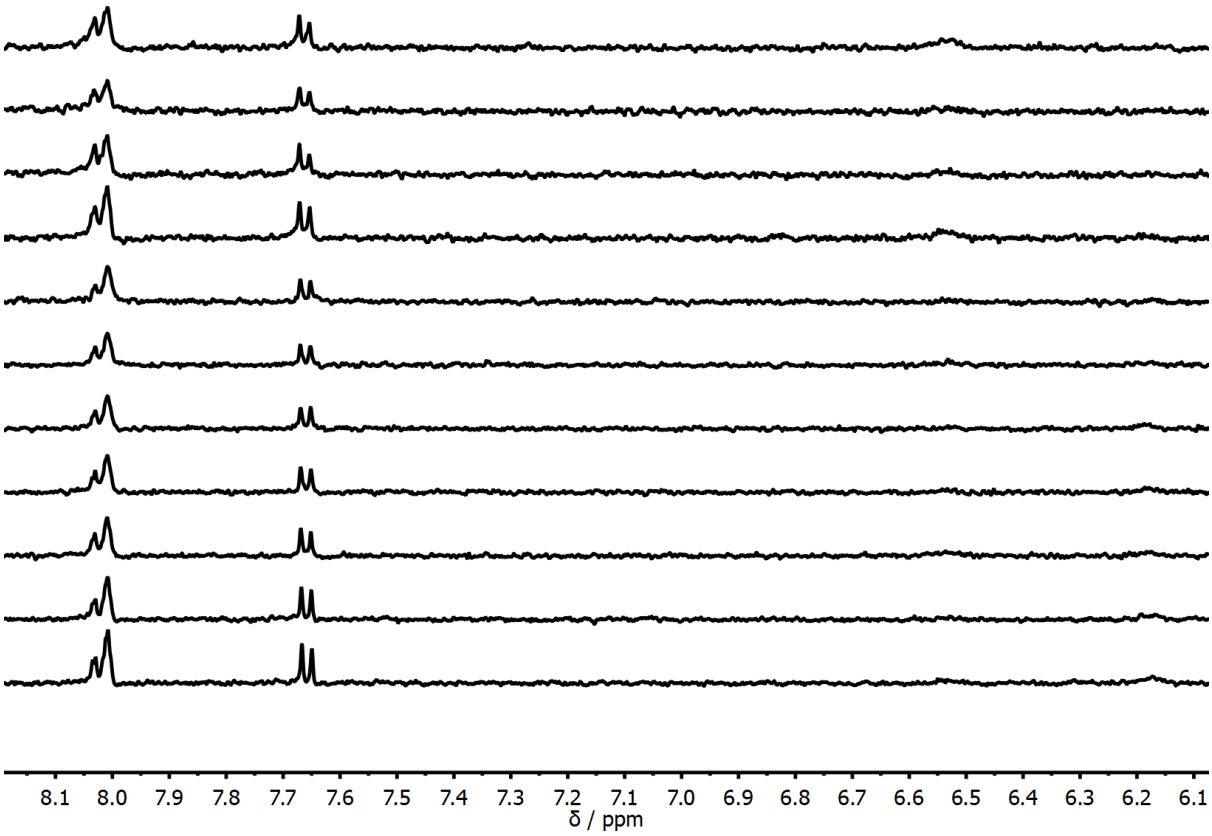

Figure S.28 – Stack plot for the NMR dilution of **1** in *n*-octane with concentration ranging from 0.314 mM (bottom) to 0.0523 mM (top).

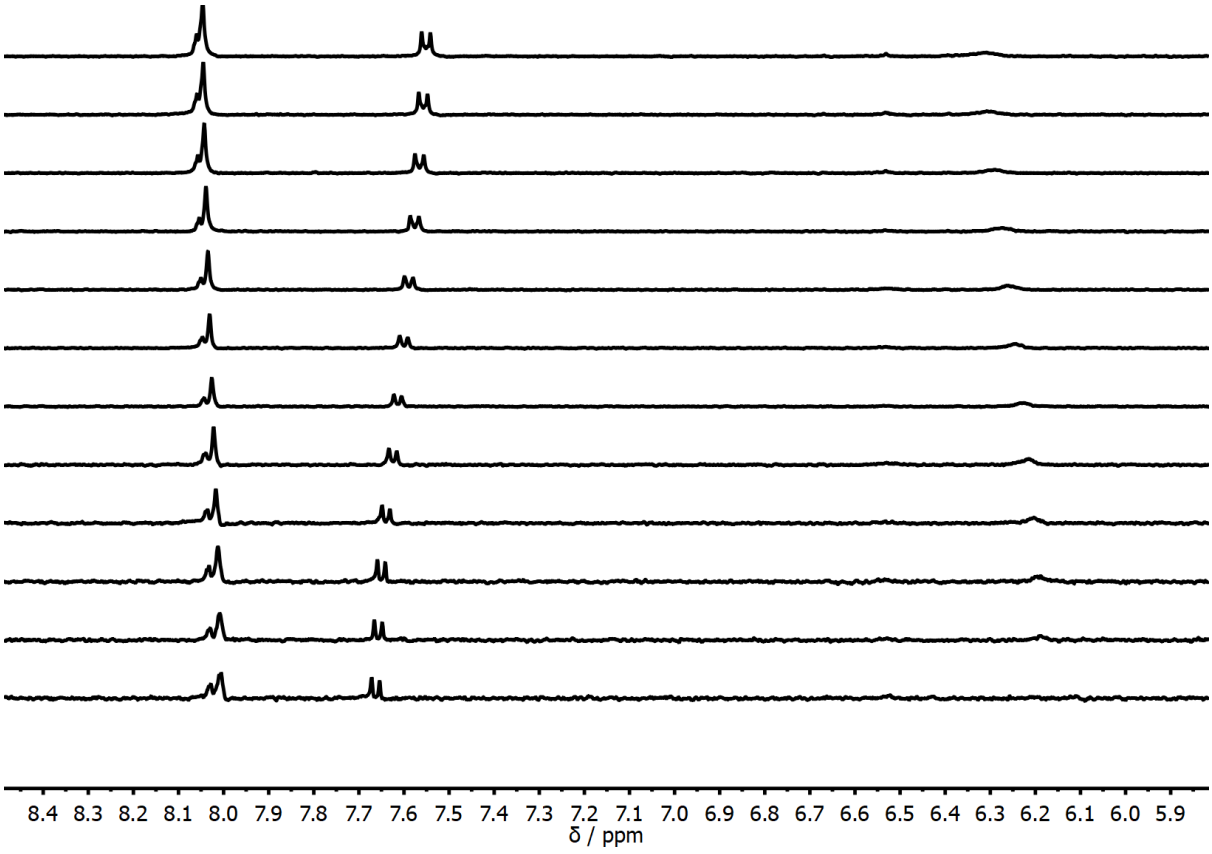

Figure S.29 – Stack plot for the NMR titration of PFTB into **1** (0.313 mM) in *n*-octane at 298 K.

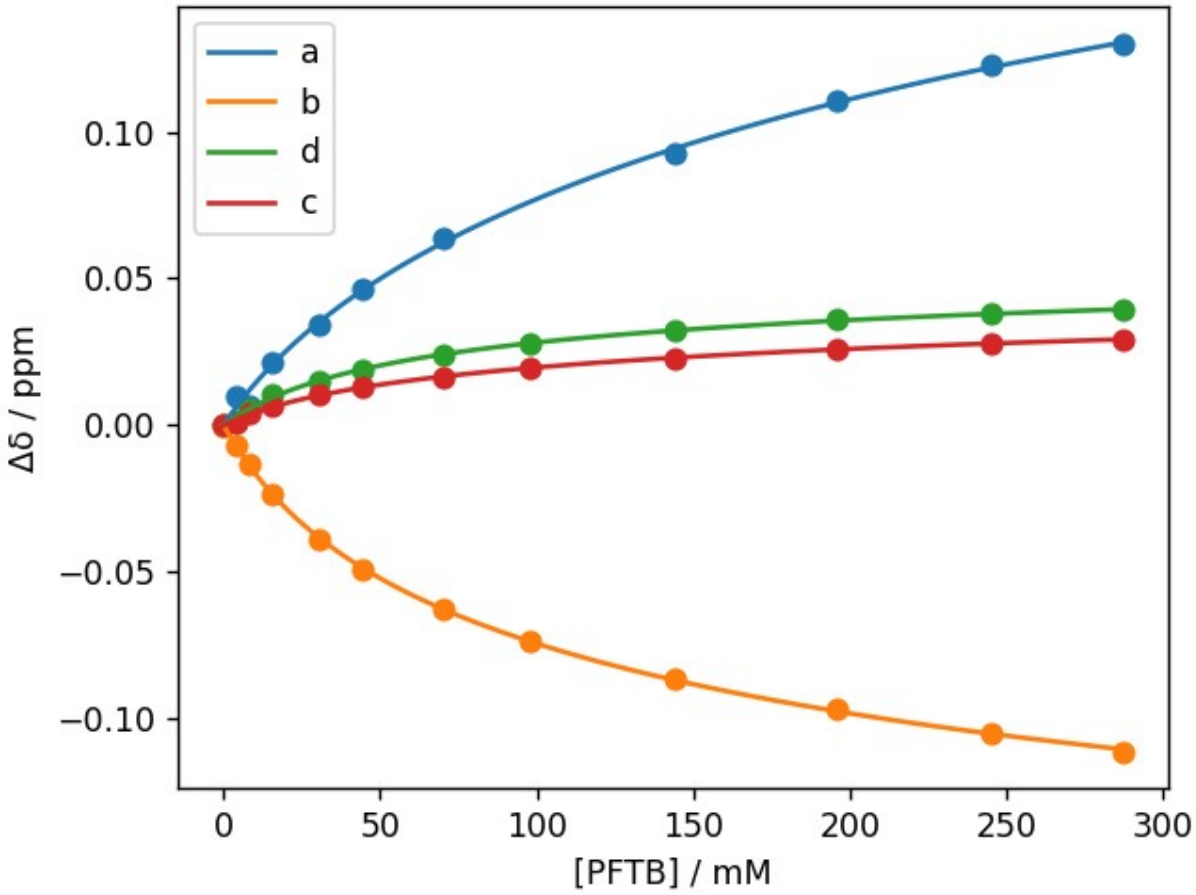

Figure S.30 – Fit for the NMR titration of PFTB into **1** (0.313 mM) to a 1:2 titration in *n*-octane at 298 K.

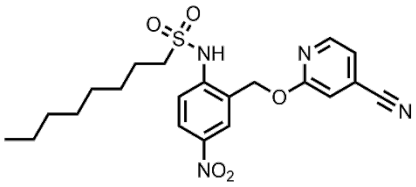

Figure S.31 – Structure of the host **3**.

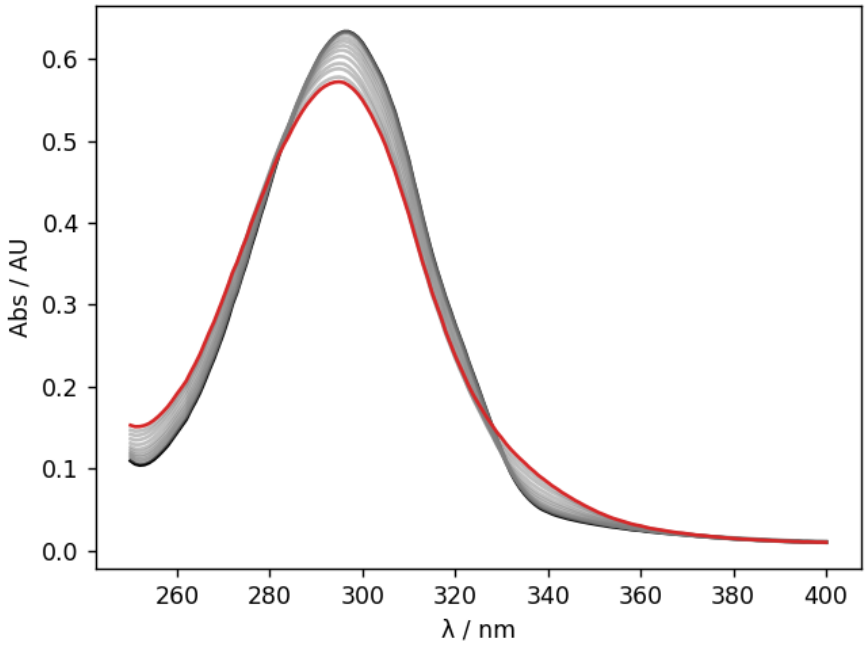

Figure S.32 - UV-vis absorption spectra for the titration of PFTB into **3** (0.0432 mM in *n*-octane, at 298K). The UV-vis spectrum of the host **3** and the final point of the titration are reported in black and in red, respectively.

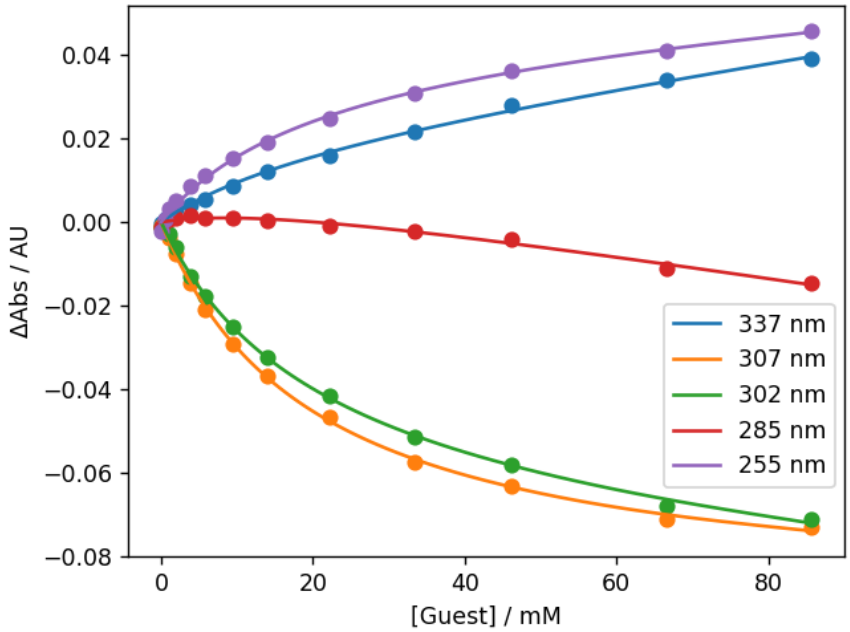

Figure S.33 - The fit of the absorbance at selected wavelengths to a 1:2 binding isotherm for the titration of PFTB into **3** (0.0432 mM in *n*-octane, at 298 K).

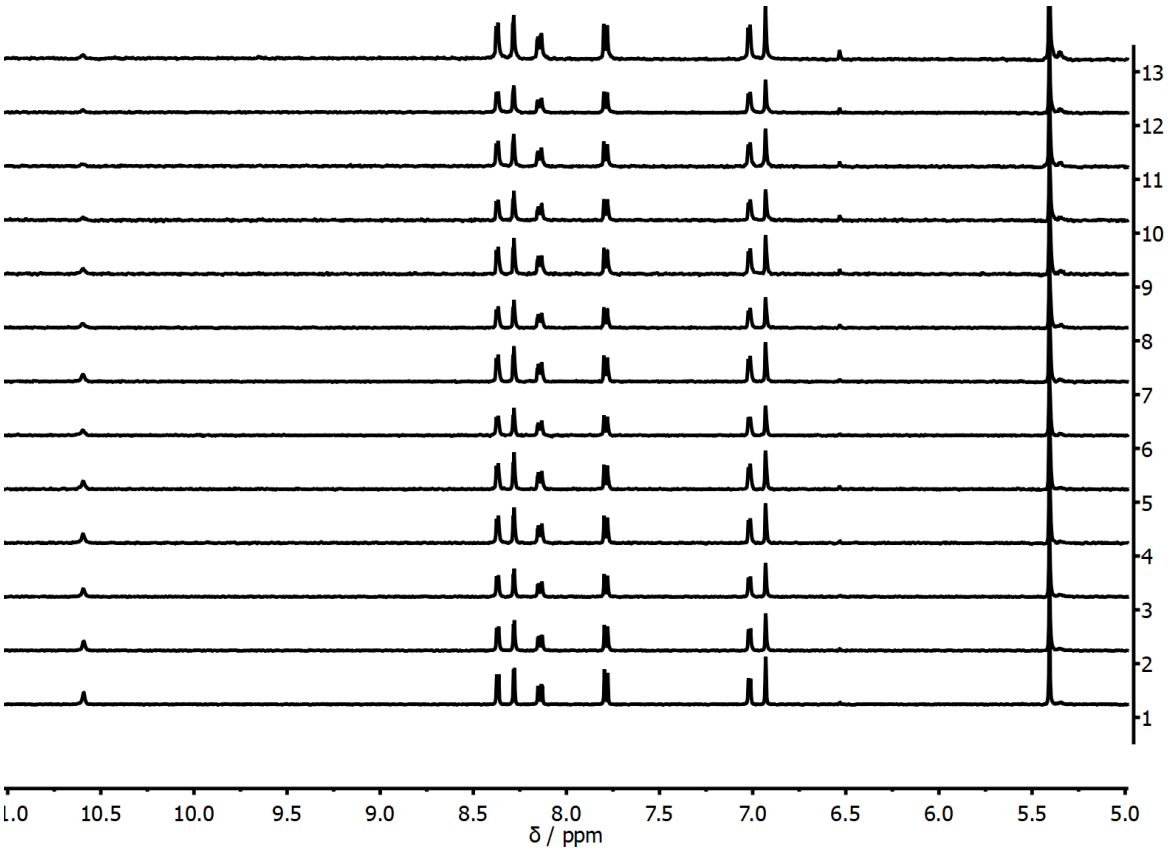

Figure S.34 – Stack plot for the NMR dilution of **3** in *n*-octane with concentration ranging from 0.721 mM (bottom) to 0.0941 mM (top).

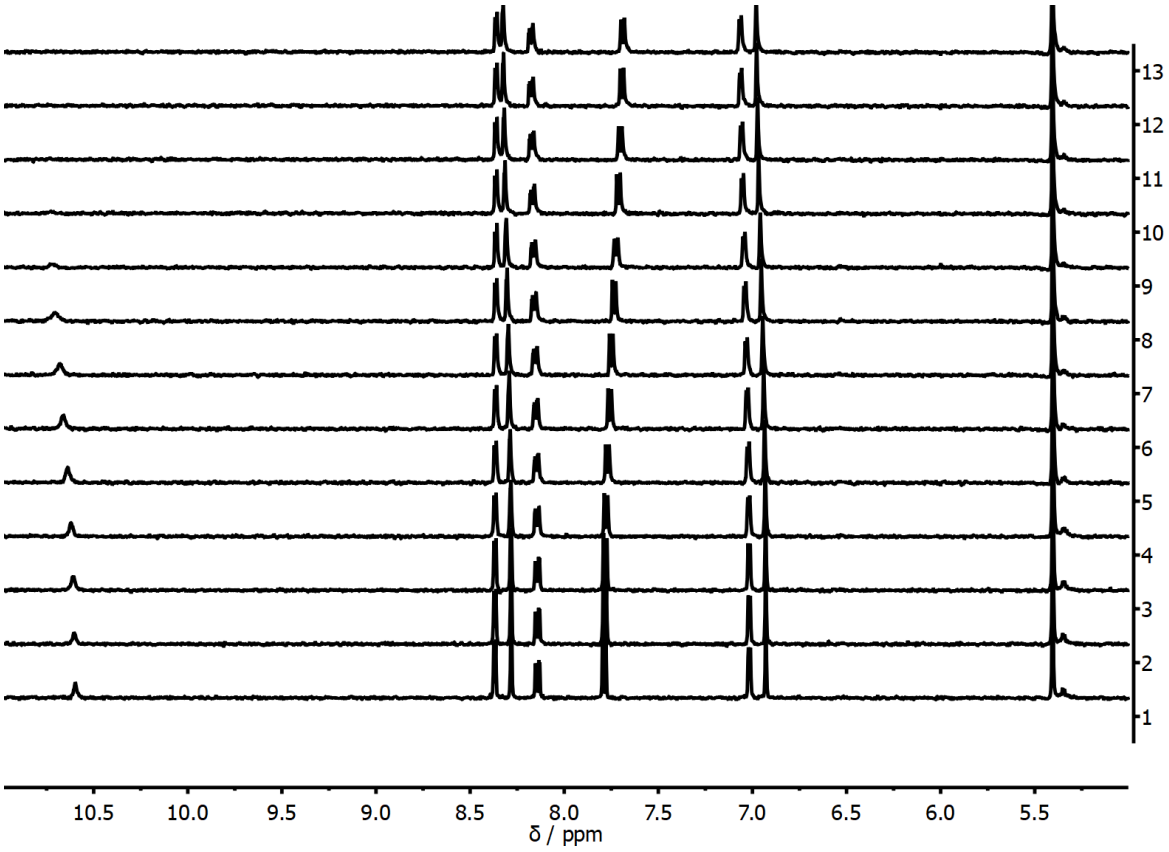

Figure S.35 – Stack plot for the NMR titration of PFTB into **3** (0.361 mM) in *n*-octane at 298 K.

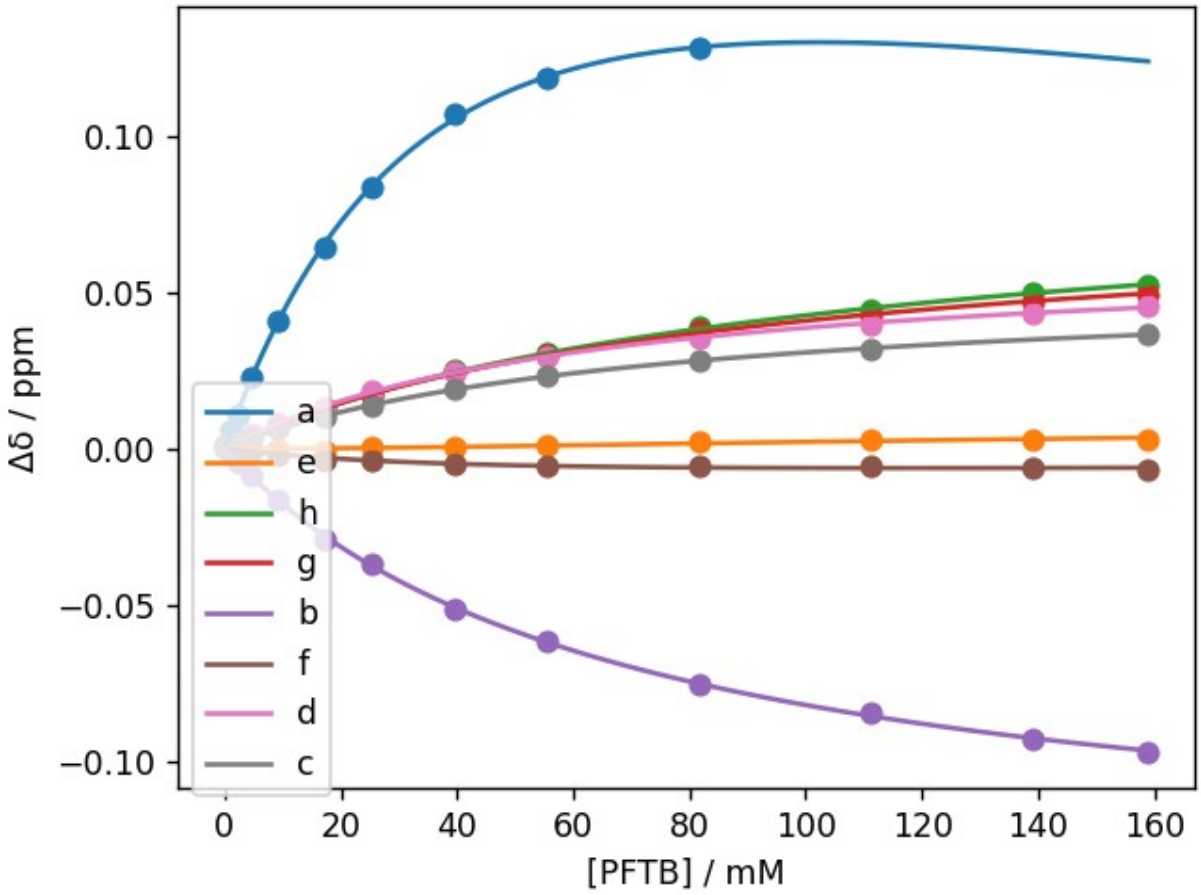

Figure S.36 – Fit for the NMR titration of PFTB into **3** (0.361 mM) to a 1:2 titration in *n*-octane at 298 K.

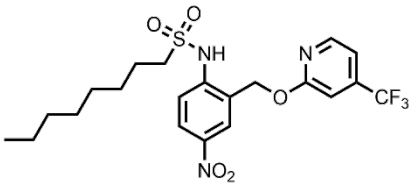

Figure S.37 – Structure of the host **4**.

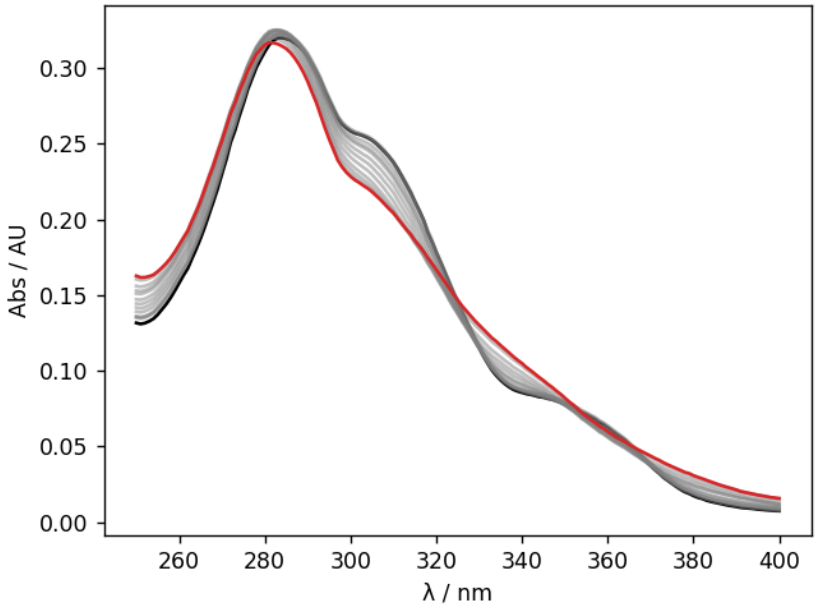

Figure S.38 - UV-vis absorption spectra for the titration of PFTB into **4** (0.0331 mM in *n*-octane, at 298K). The UV-vis spectrum of the host **2** and the final point of the titration are reported in black and in red, respectively.

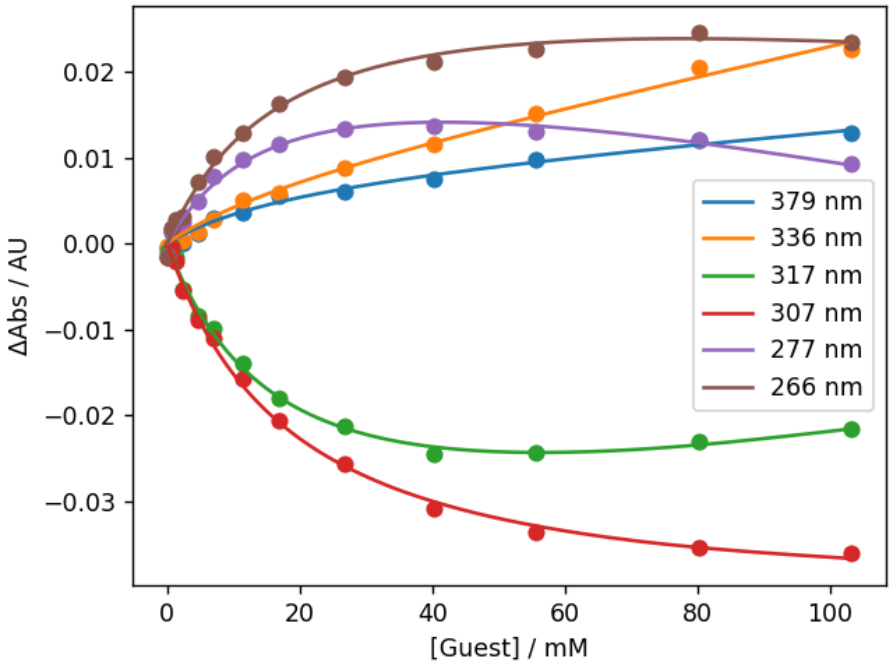

Figure S.39 - The fit of the absorbance at selected wavelengths to a 1:2 binding isotherm of PFTB into **4** (0.0331 mM in *n*-octane, at 298 K).

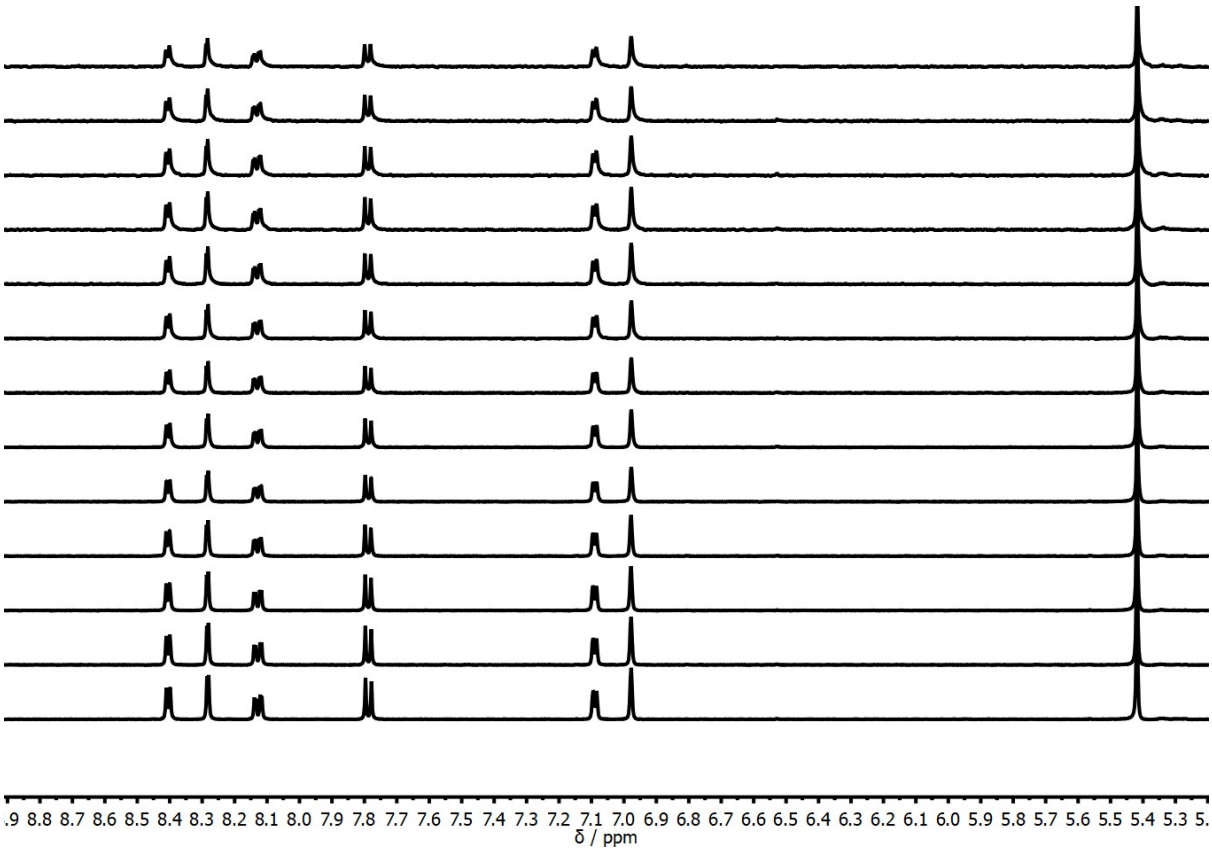

Figure S.40 – Stack plot for the NMR dilution of **4** in *n*-octane with concentration ranging from 1.79 mM (bottom) to 0.256 mM (top).

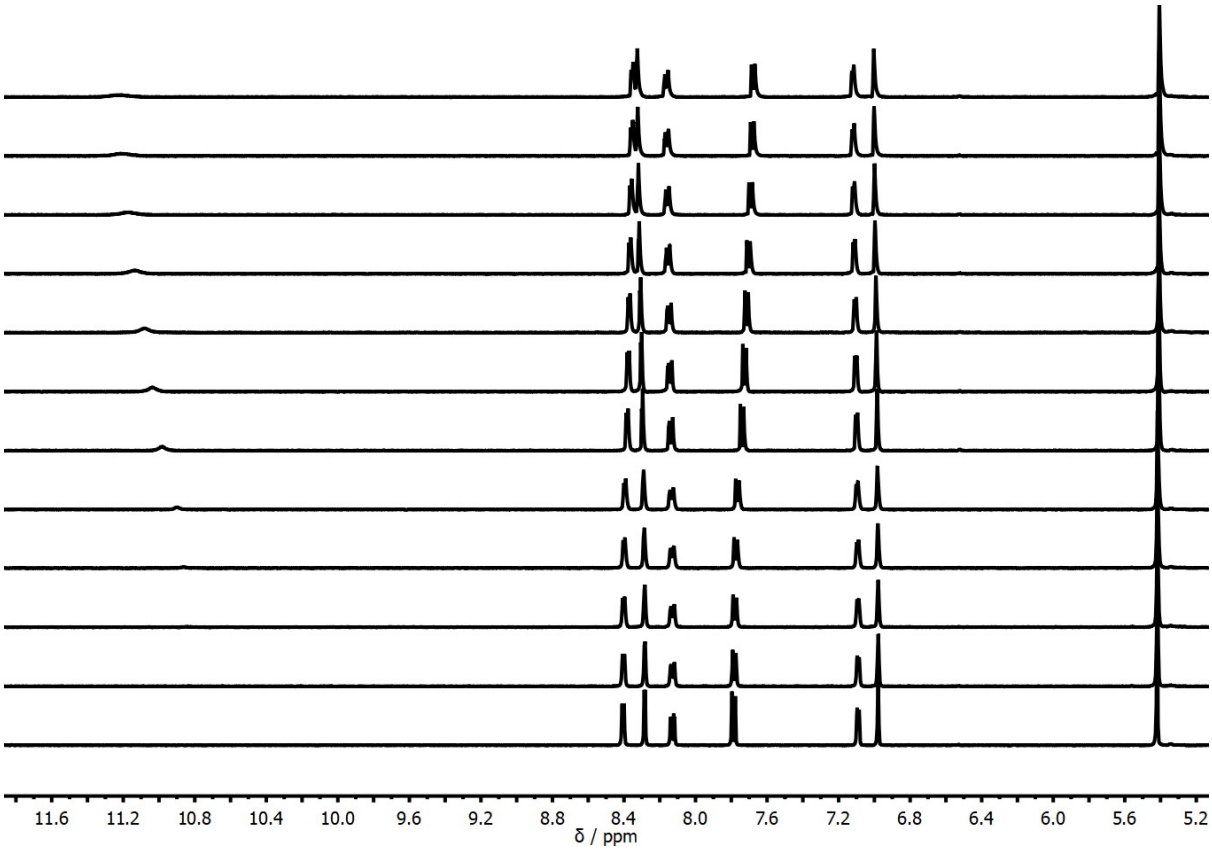

Figure S.41 – Stack plot for the NMR titration of PFTB into **4** (1.79 mM) in *n*-octane at 298 K.

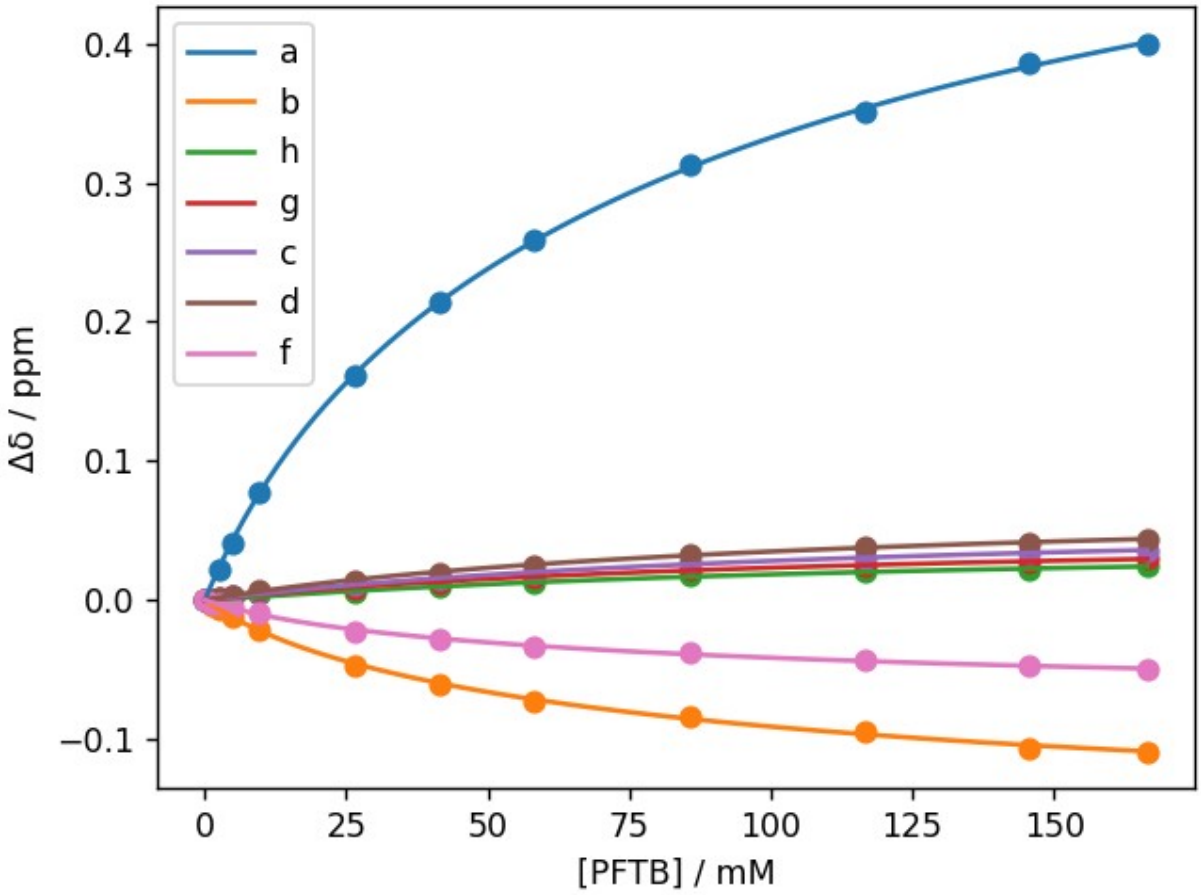

Figure S.42 – Fit for the NMR titration of PFTB into **4** (1.79 mM) to a 1:2 titration in *n*-octane at 298 K.

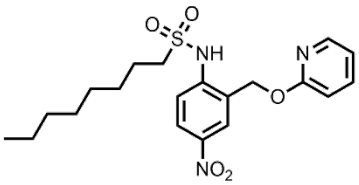

Figure S.43 – Structure of the host **5**.

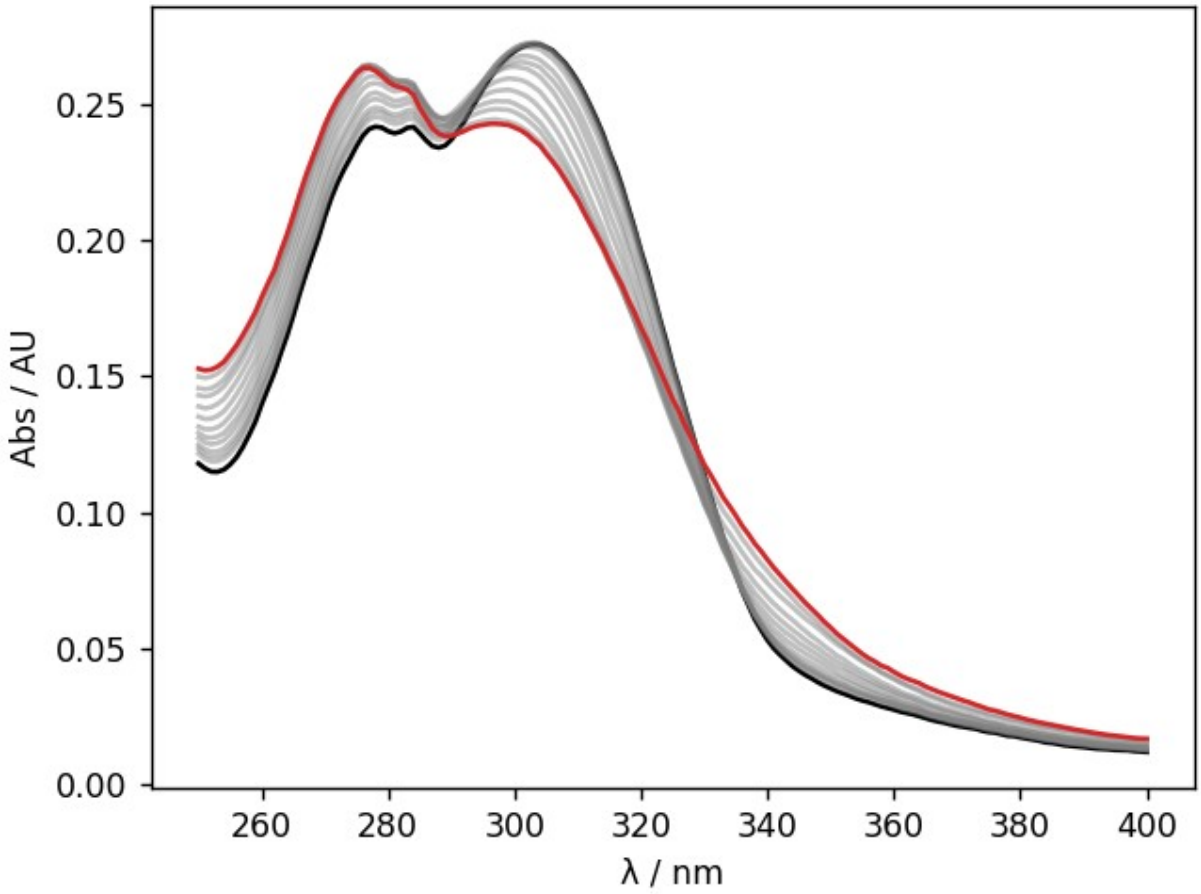

Figure S.44 - UV-vis absorption spectra for the titration of PFTB into **2** (0.0278 mM in *n*-octane, at 298K). The UV-vis spectrum of the host **2** and the final point of the titration are reported in black and in red, respectively.

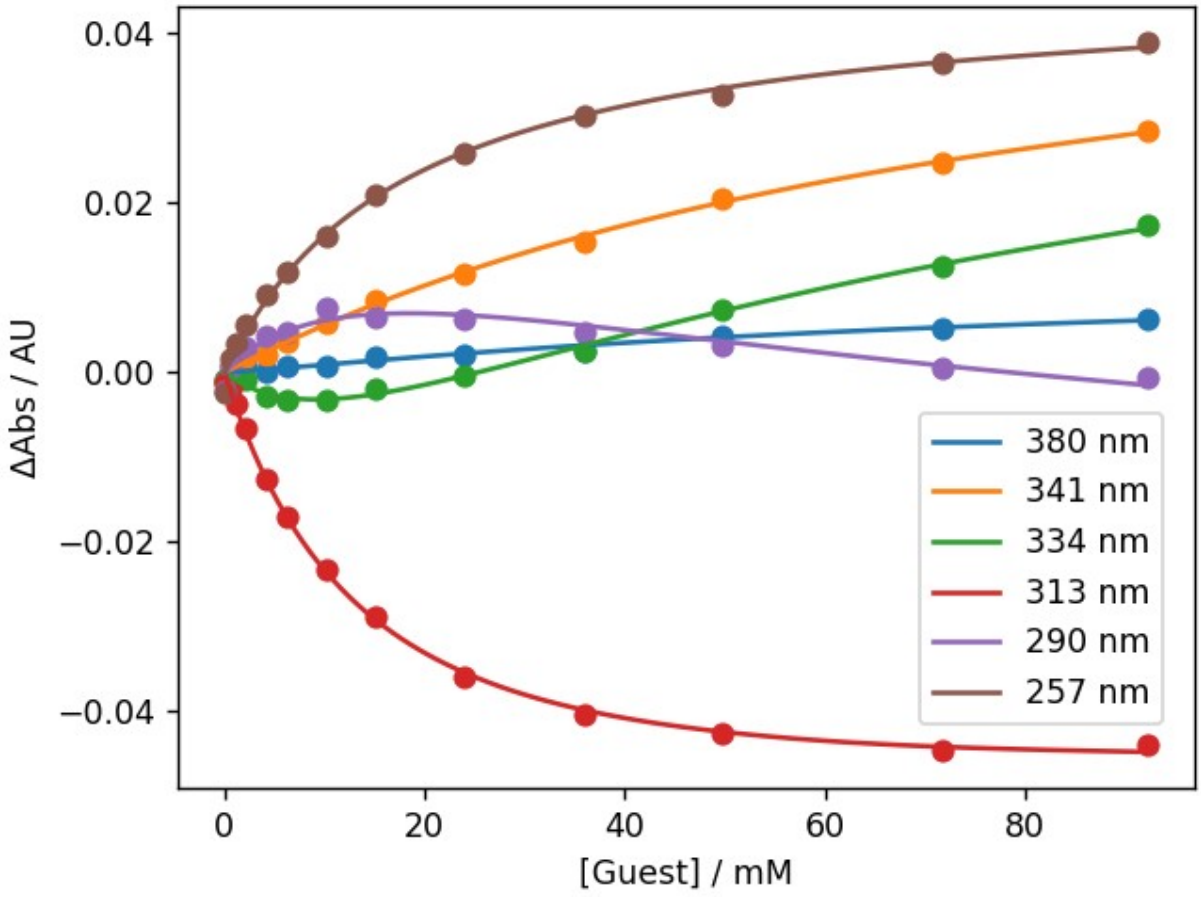

Figure S.45 - The fit of the absorbance at selected wavelengths to a 1:2 binding isotherm for the titration of PFTB into **2** (0.0278 mM in *n*-octane, at 298 K). Figure S.70 – Stack plot for the NMR dilution of **12** in *n*-octane with concentration ranging from 0.695 mM (bottom) to 0.130 mM (top).

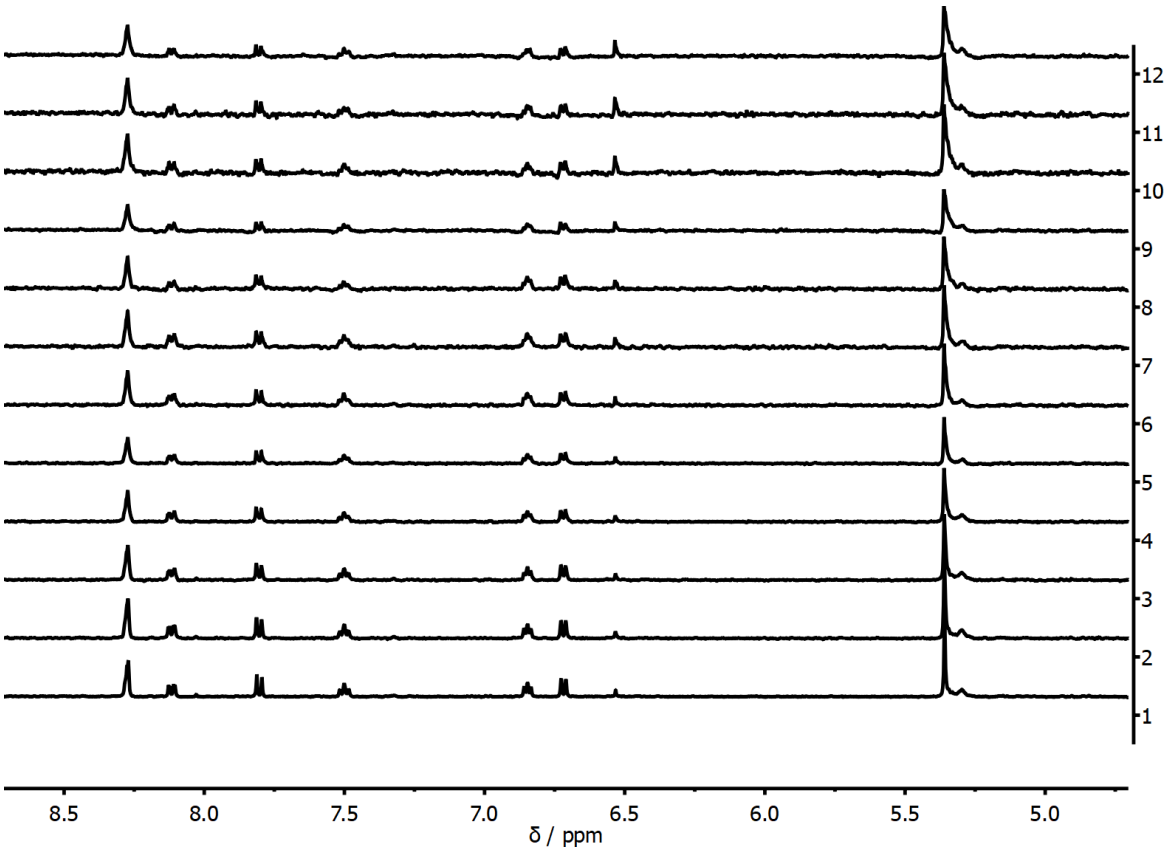

Figure S.46 – Stack plot for the NMR dilution of **5** in *n*-octane with concentration ranging from 1.28 mM (bottom) to 0.167 mM (top).

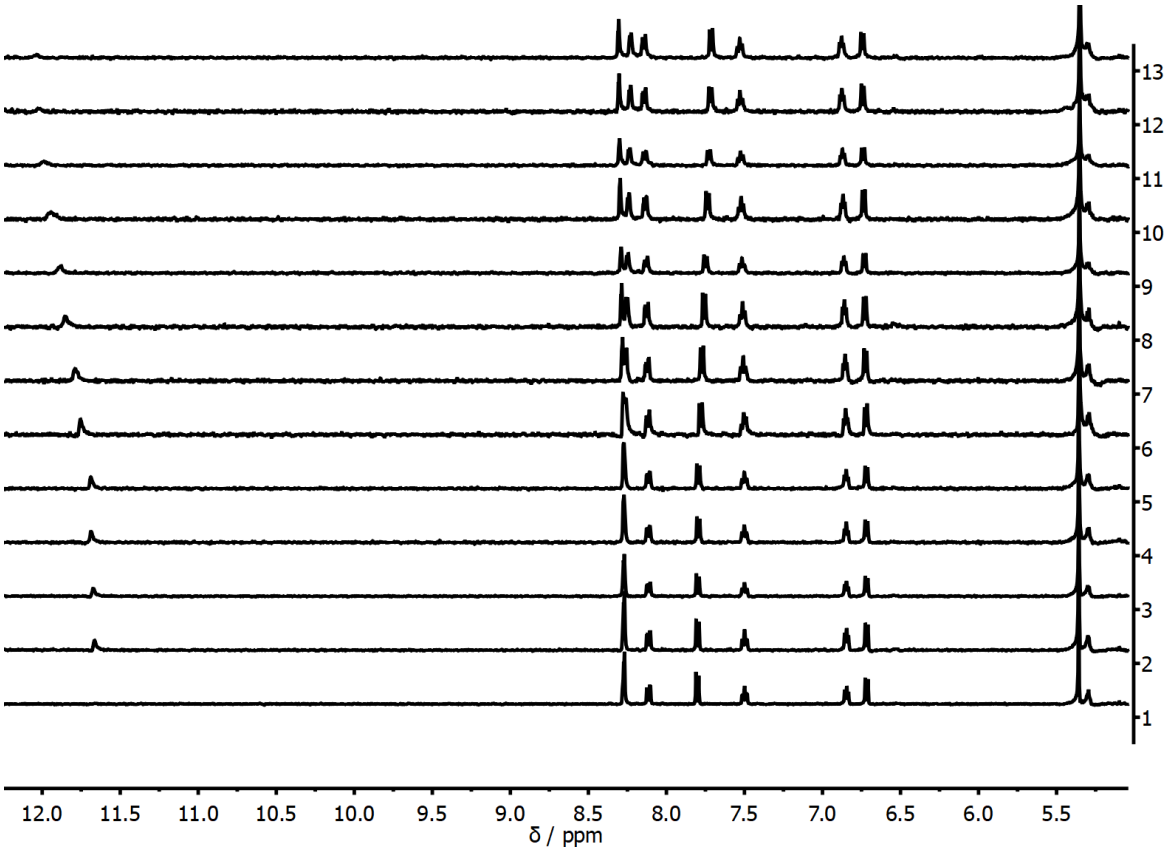

Figure S.47 – Stack plot for the NMR titration of PFTB into **5** (0.223 mM) in *n*-octane at 298 K.

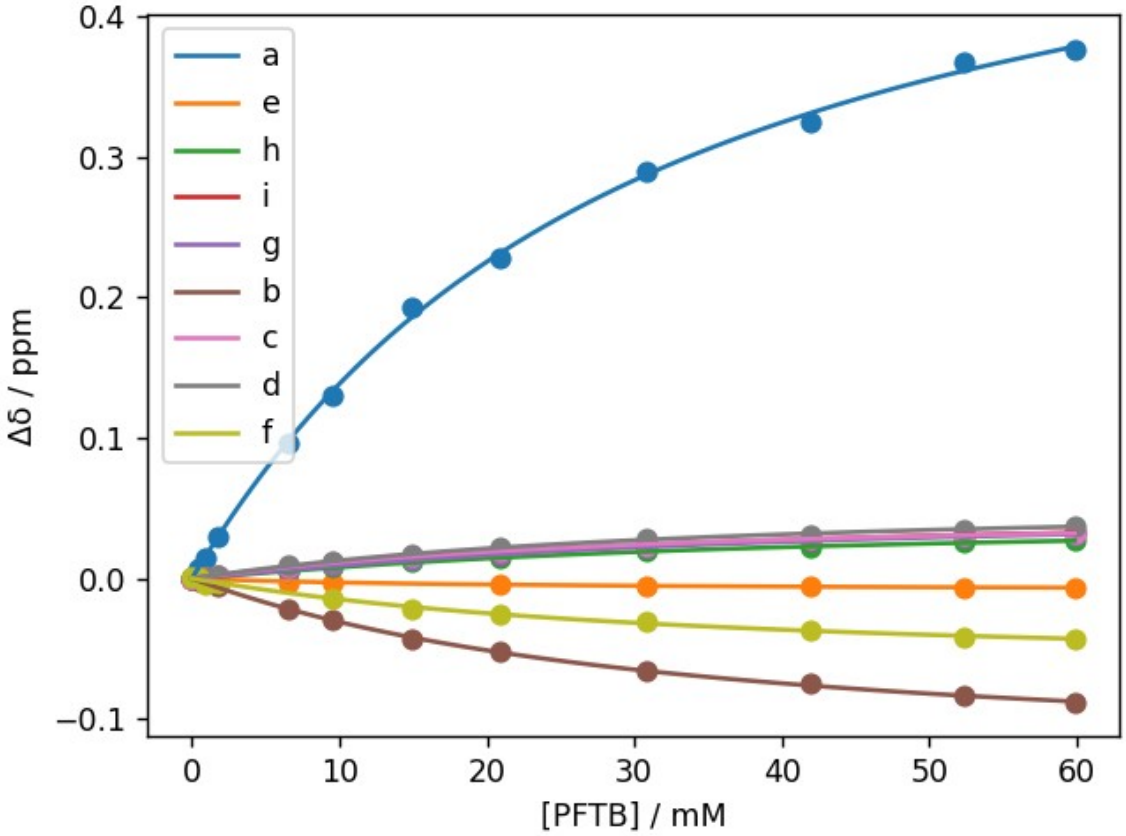

Figure S.48 – Fit for the NMR titration of PFTB into **5** (0.223 mM) to a 1:2 titration in *n*-octane at 298 K.

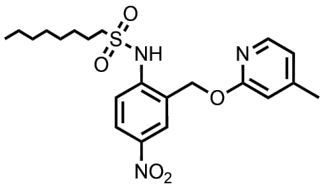

Figure S.49 – Structure of the host **6**.

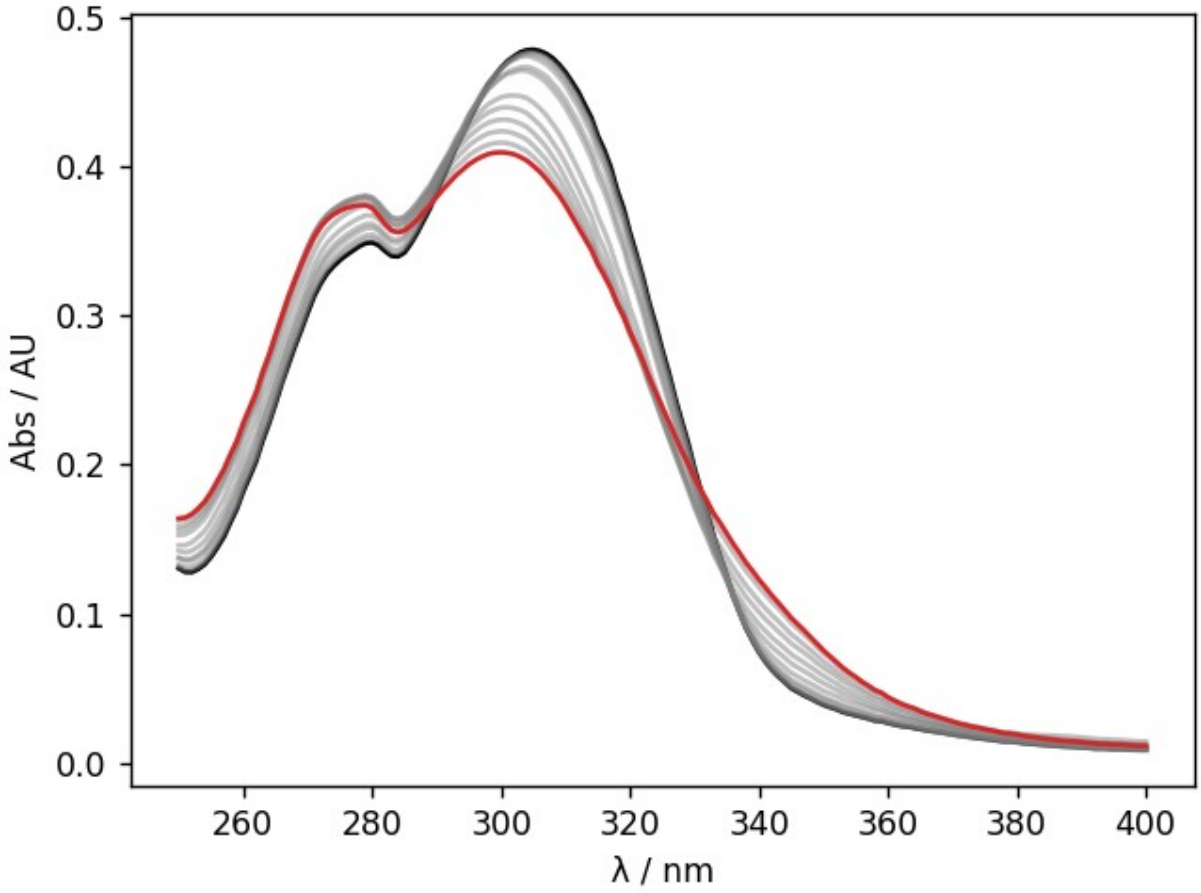

Figure S.50 - UV-vis absorption spectra for the titration of PFTB into **6** (0.0409 mM in *n*-octane, at 298K). The UV-vis spectrum of the host **6** and the final point of the titration are reported in black and in red, respectively.

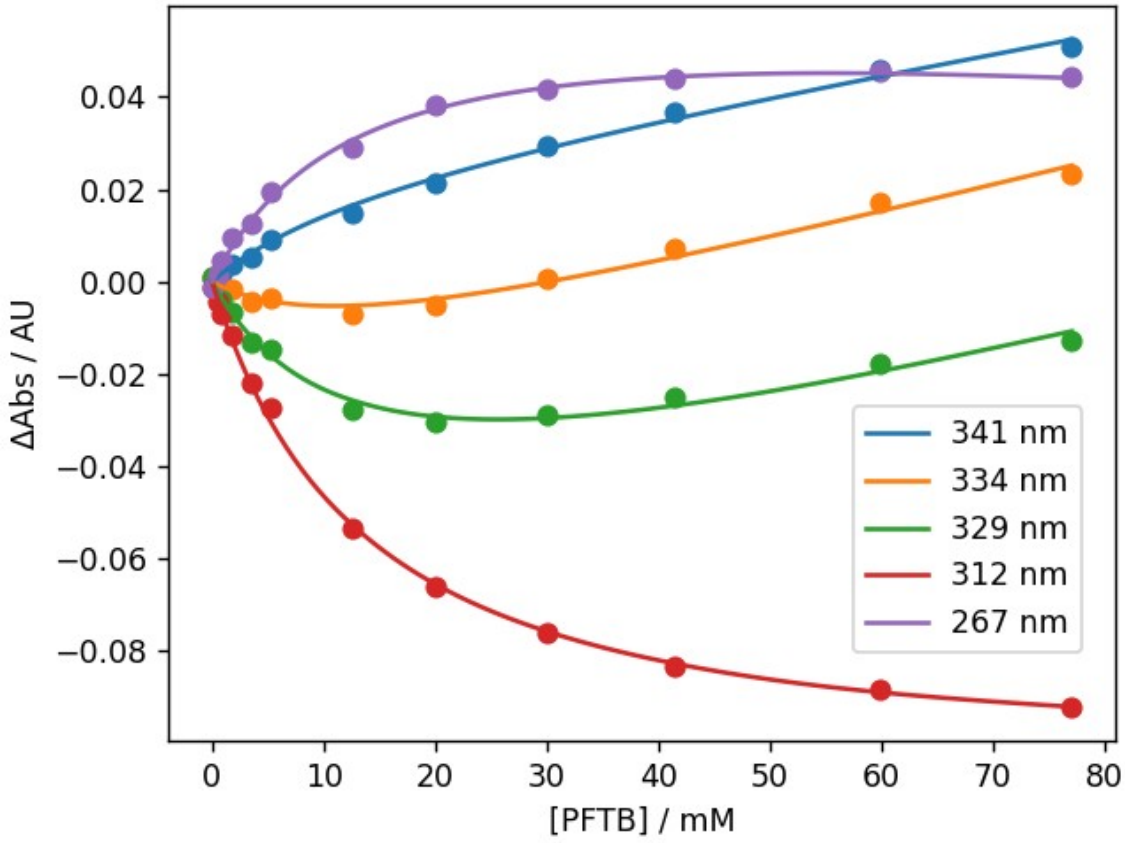

Figure S.51 - The fit of the absorbance at selected wavelengths to a 1:2 binding isotherm for the titration of PFTB into **6** (0.0409 mM in *n*-octane, at 298 K).

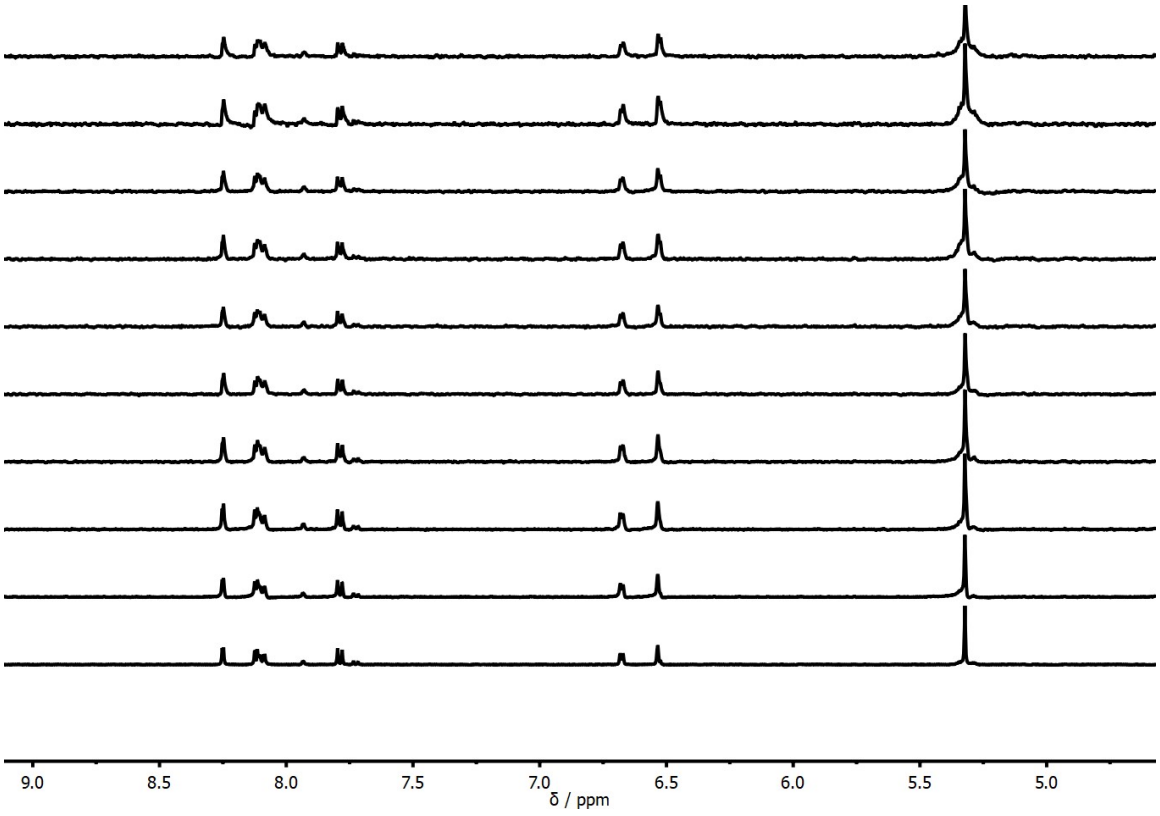

Figure S.52 – Stack plot for the NMR dilution of **6** in *n*-octane with concentration ranging from 0.409 mM (bottom) to 0.0533 mM (top).

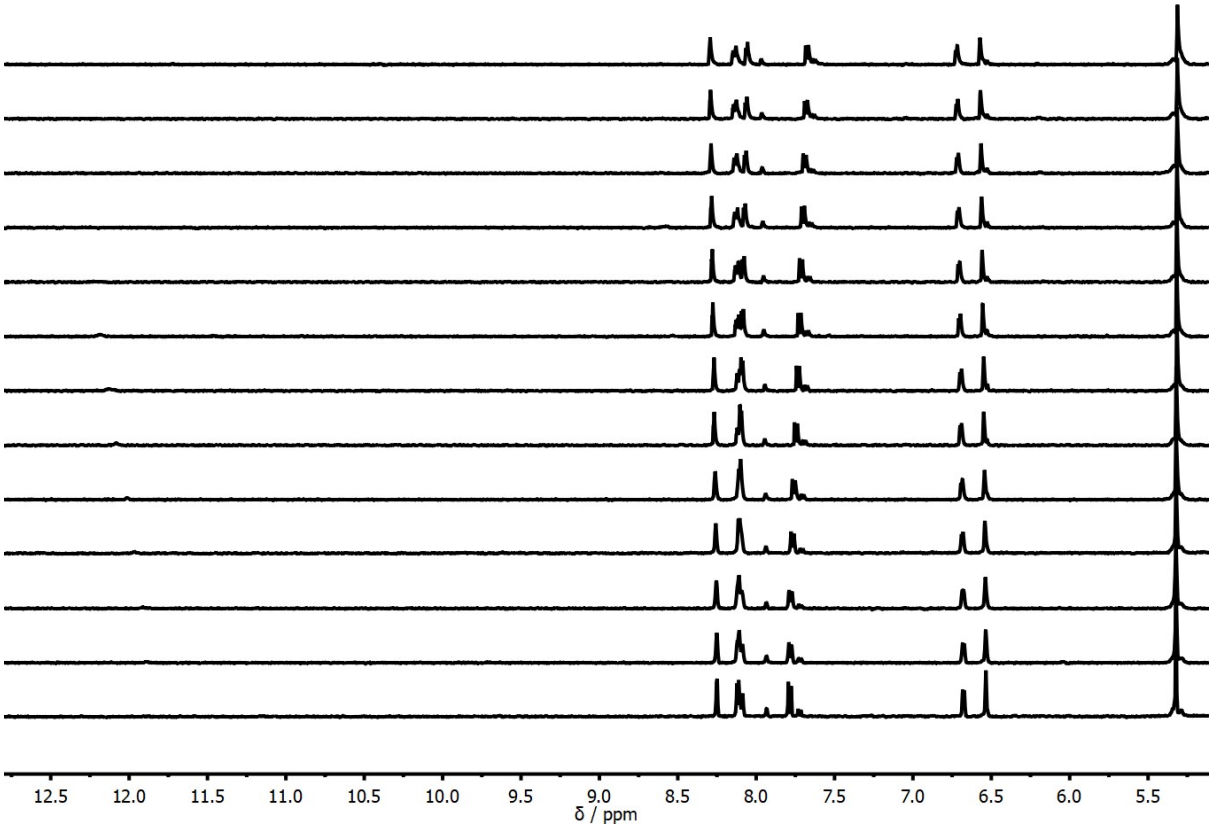

Figure S.53 – Stack plot for the NMR titration of PFTB into **6** (0.409 mM) in *n*-octane at 298 K.

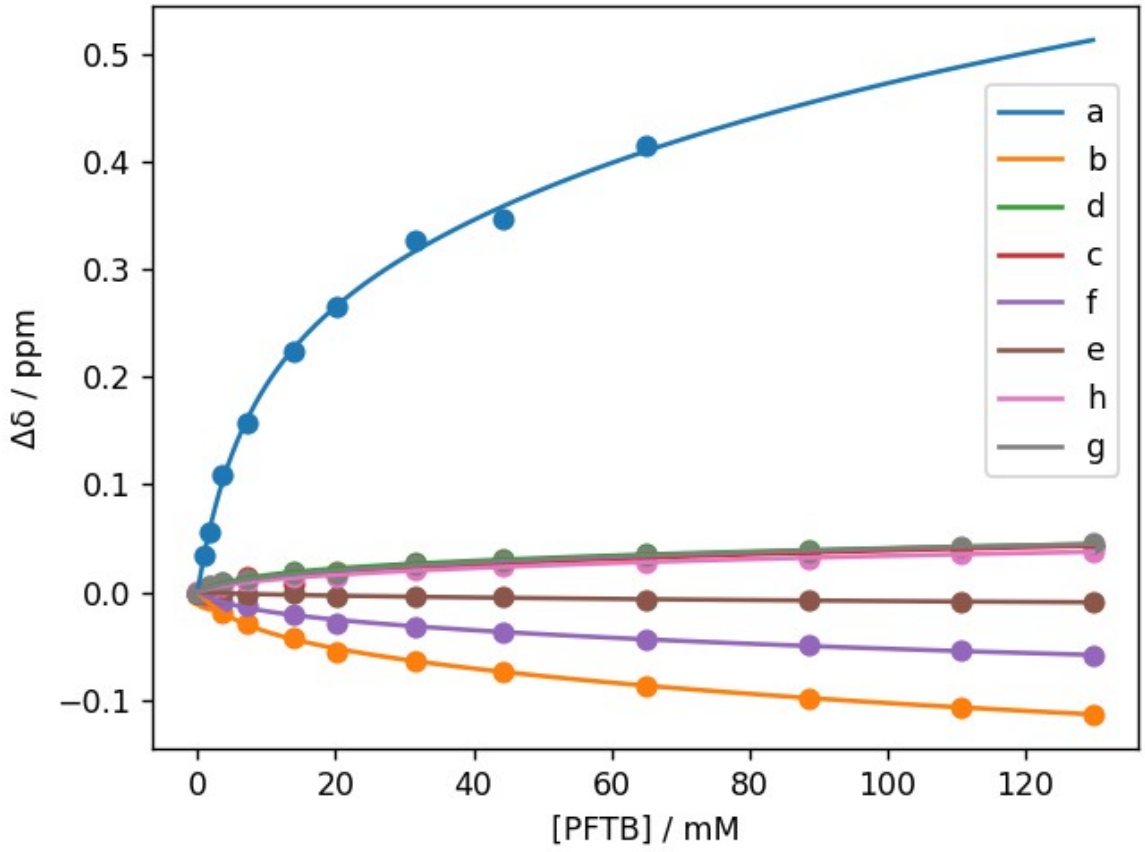

Figure S.54 – Fit for the NMR titration of PFTB into **6** (0.409 mM) to a 1:2 titration in *n*-octane at 298 K.

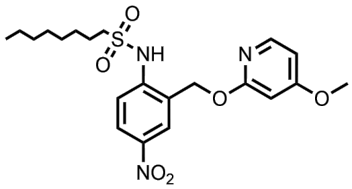

Figure S.55 – Structure of the host **7**.

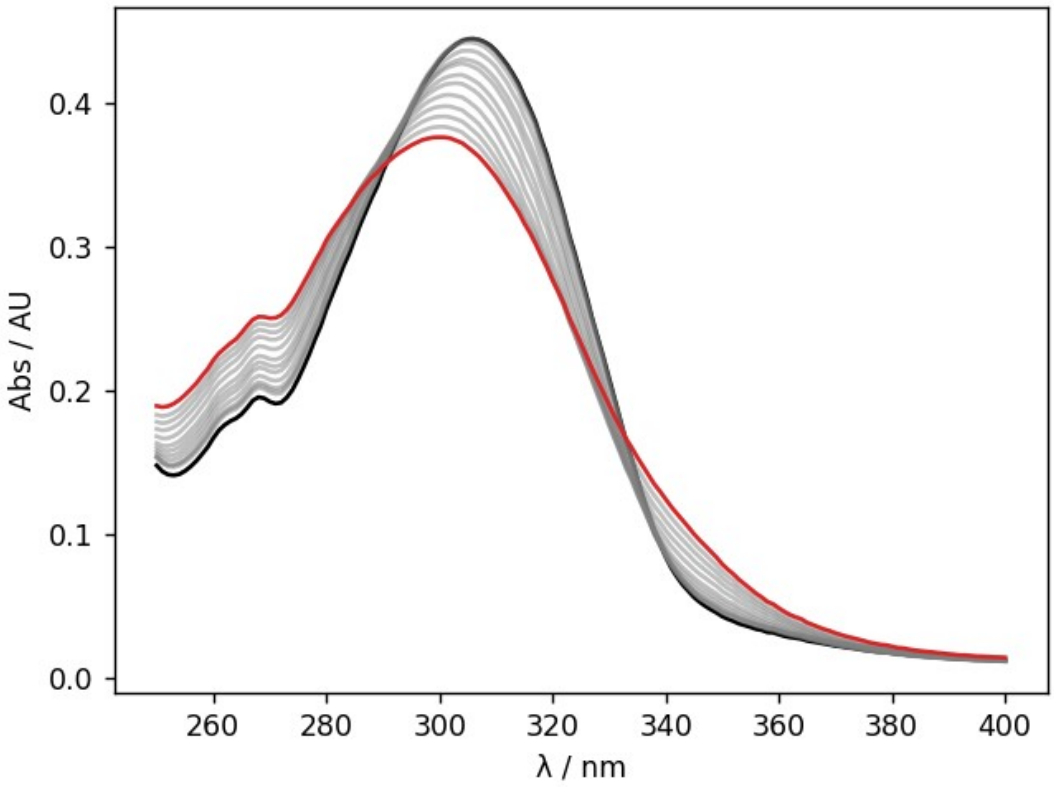

Figure S.56 - UV-vis absorption spectra for the titration of PFTB into **6** (0.0322 mM in *n*-octane, at 298K). The UV-vis spectrum of the host **7** and the final point of the titration are reported in black and in red, respectively.

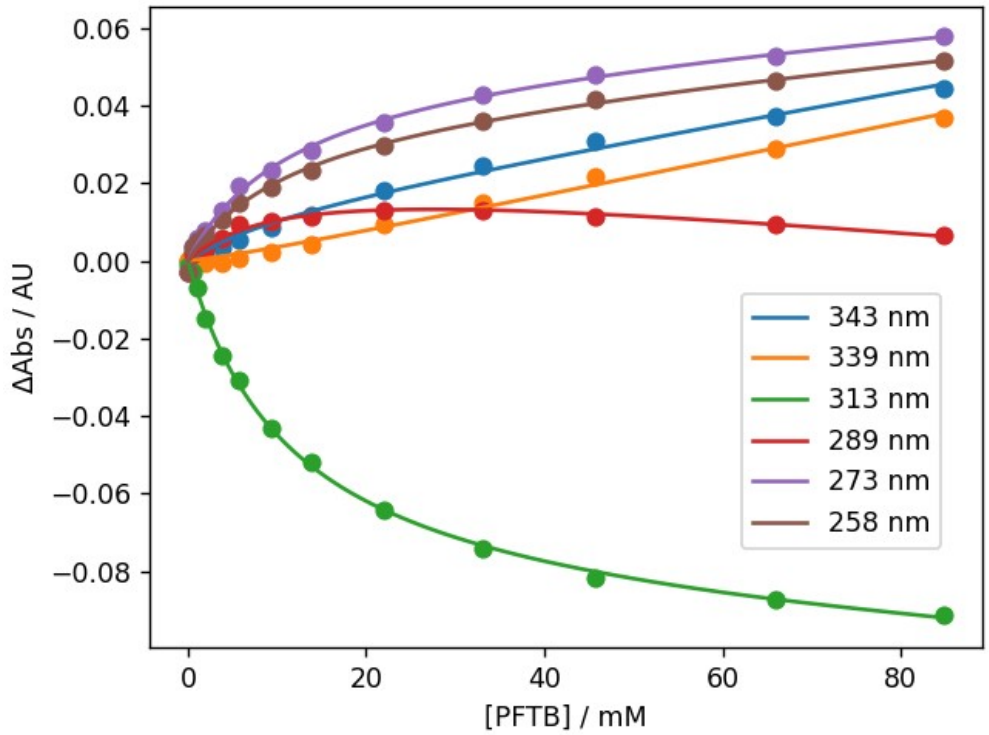

Figure S.57 - The fit of the absorbance at selected wavelengths to a 1:2 binding isotherm for the titration of PFTB into **7** (0.0322 mM in *n*-octane, at 298 K).

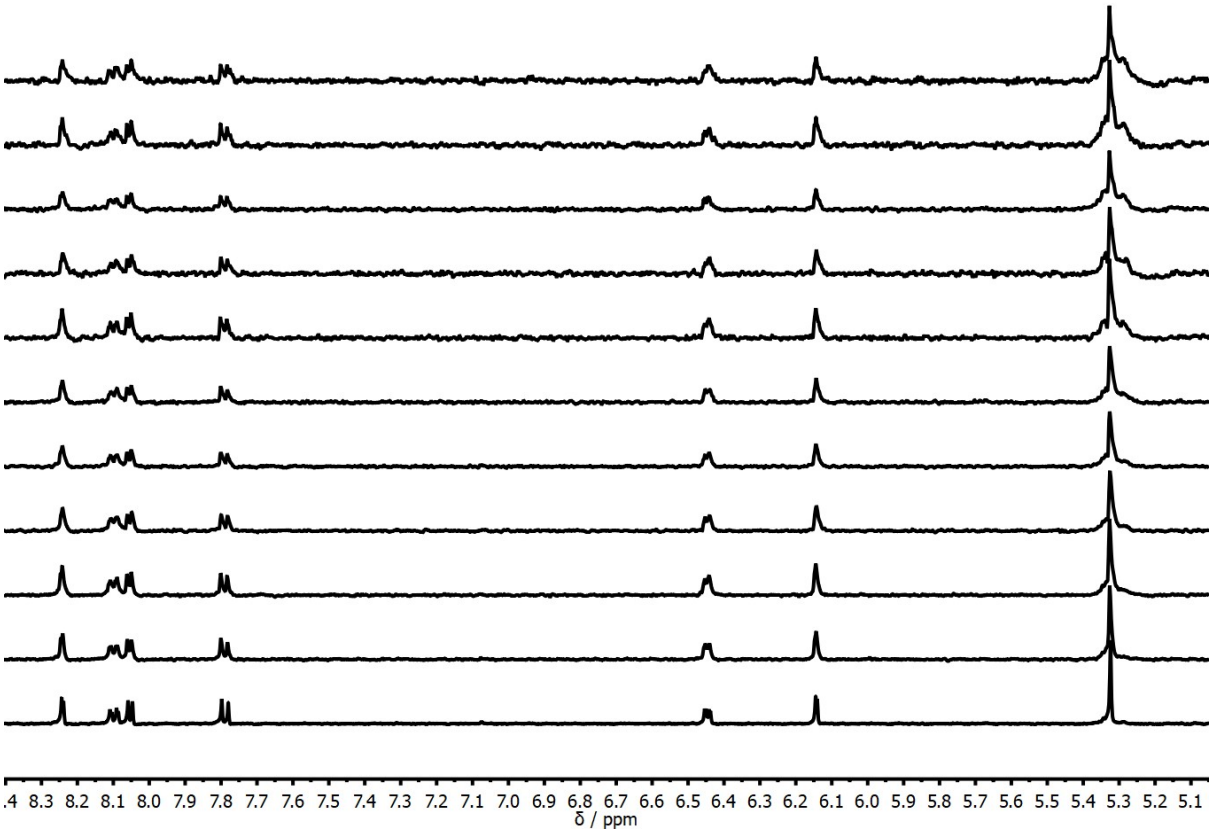

Figure S.58 – Stack plot for the NMR dilution of **7** in *n*-octane with concentration ranging from 0.202 mM (bottom) to 0.0316 mM (top).

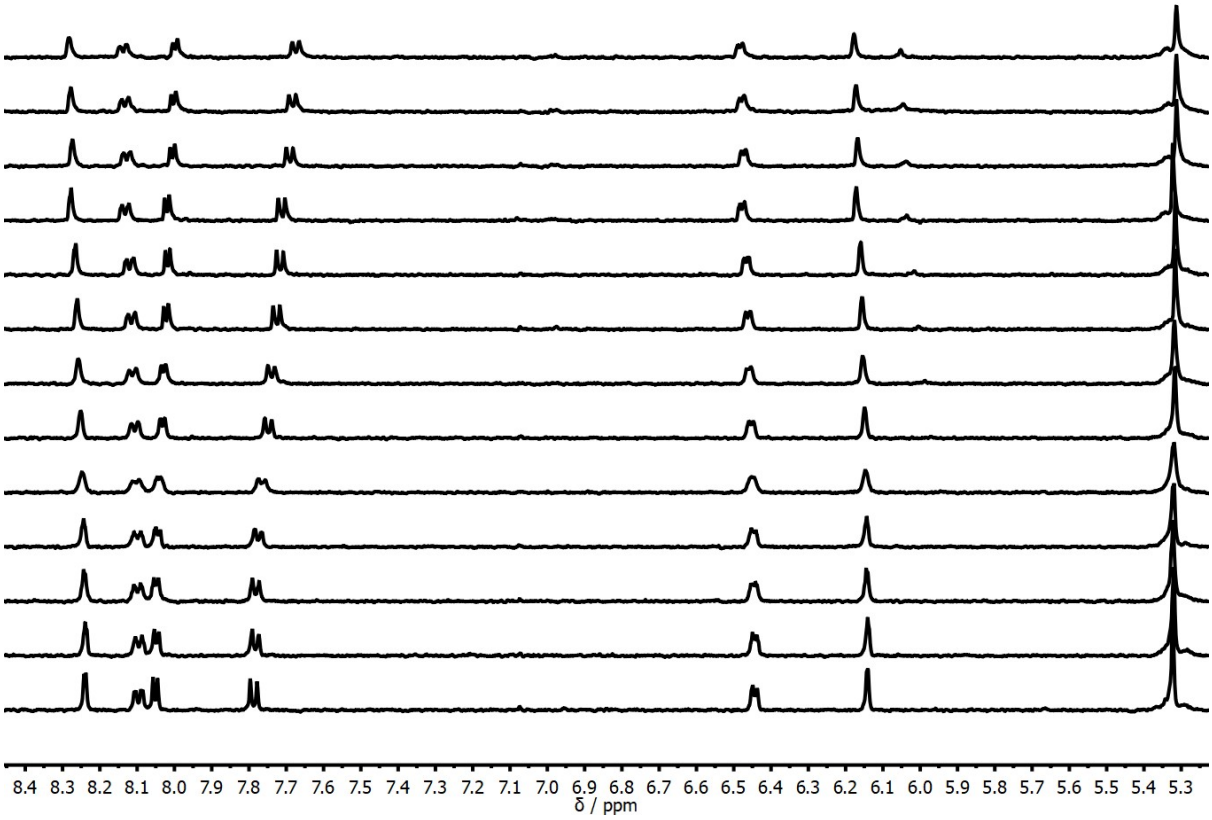

Figure S.59 – Stack plot for the NMR titration of PFTB into **7** (0.202 mM) in *n*-octane at 298 K.

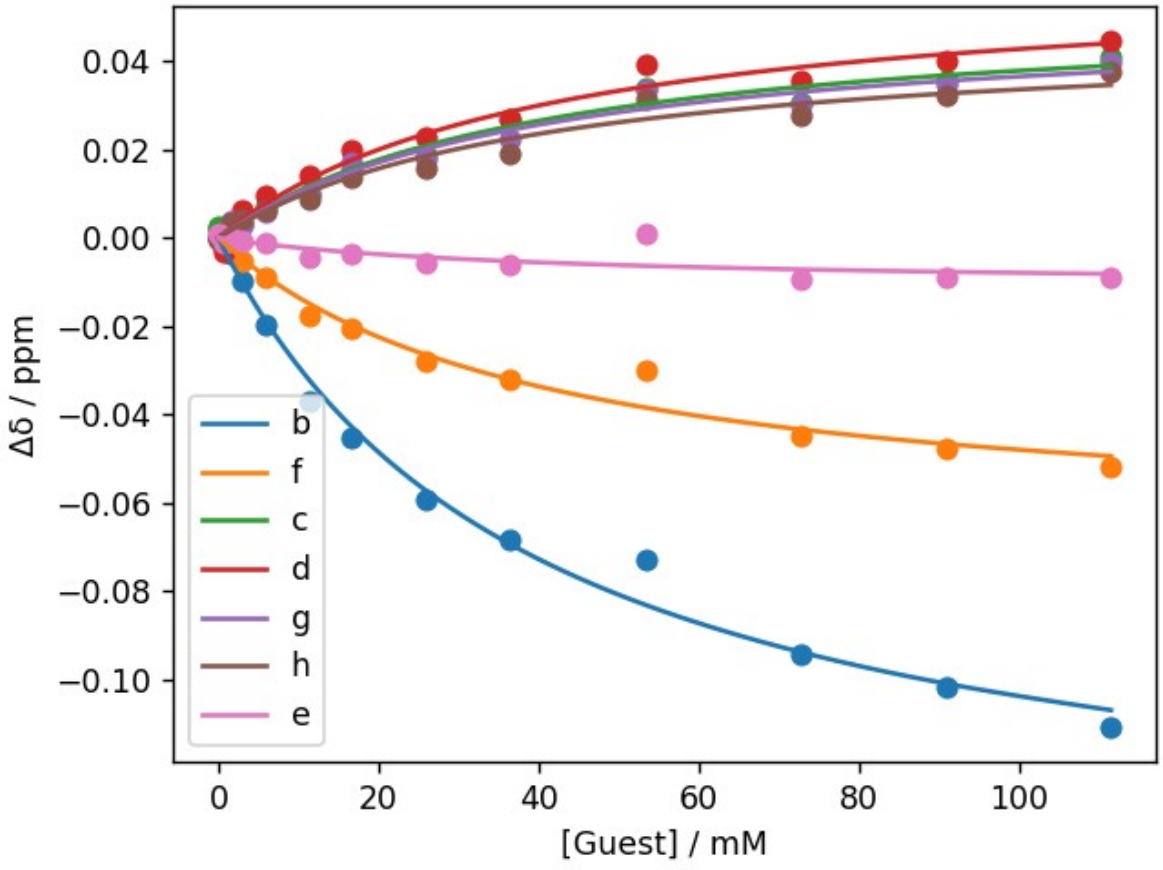

Figure S.60 – Fit for the NMR titration of PFTB into **7** (0.202 mM) to a 1:2 titration in *n*-octane at 298 K.

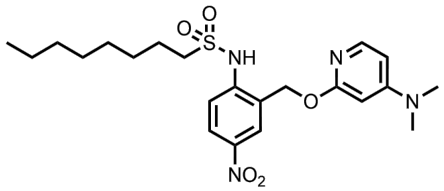

Figure S.61 – Structure of the host **8**

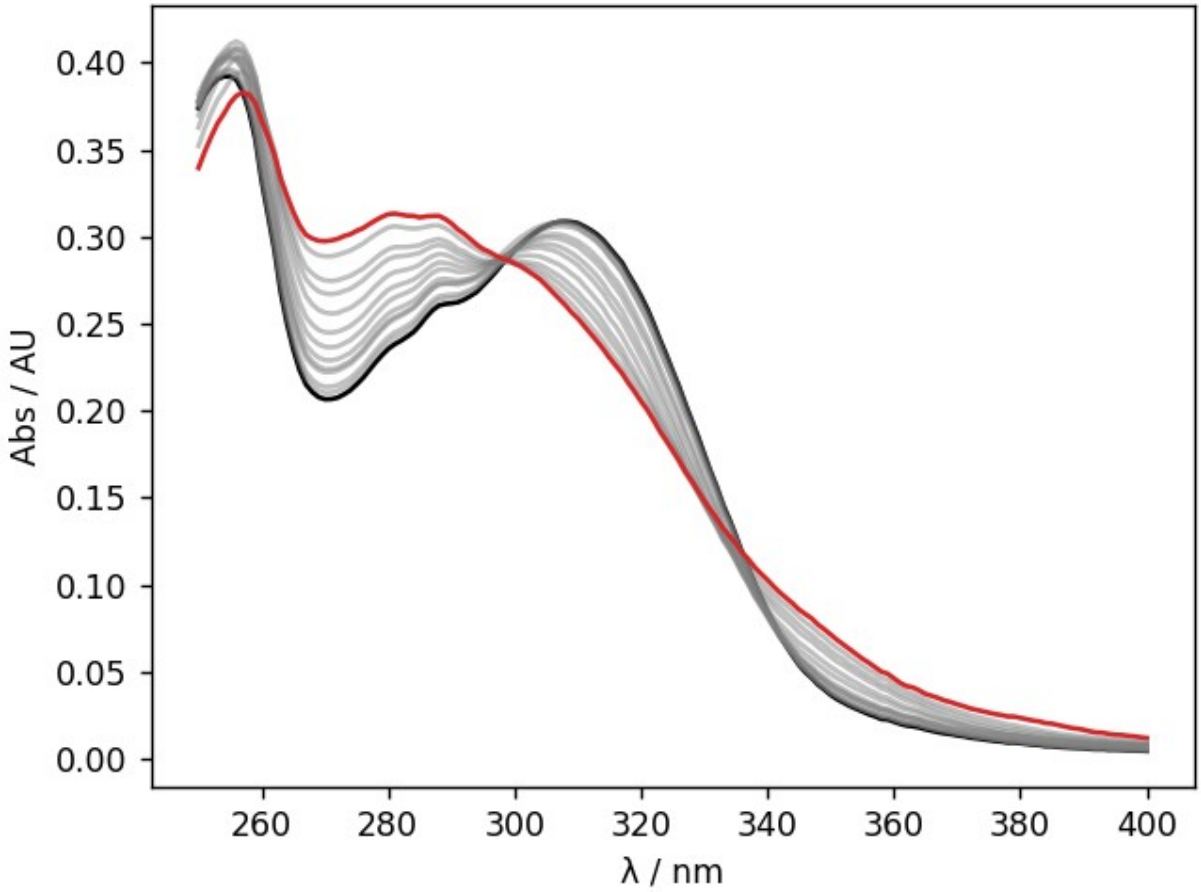

Figure S.62 - UV-vis absorption spectra for the titration of PFTB into **8** (0.0265 mM in *n*-octane, at 298K). The UV-vis spectrum of the host **8** and the final point of the titration are reported in black and in red, respectively.

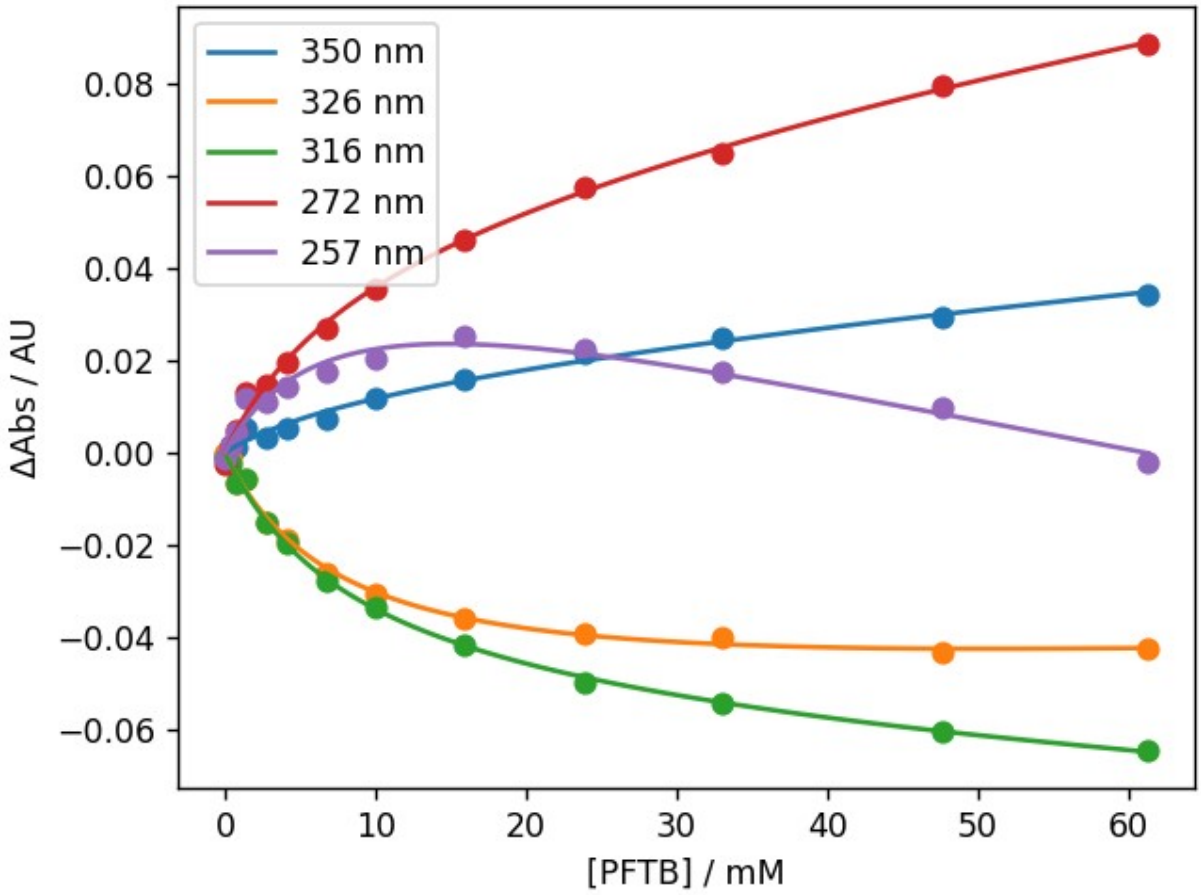

Figure S.63 - The fit of the absorbance at selected wavelengths to a 1:2 binding isotherm for the titration of PFTB into **8** (0.0265 mM in *n*-octane, at 298 K).

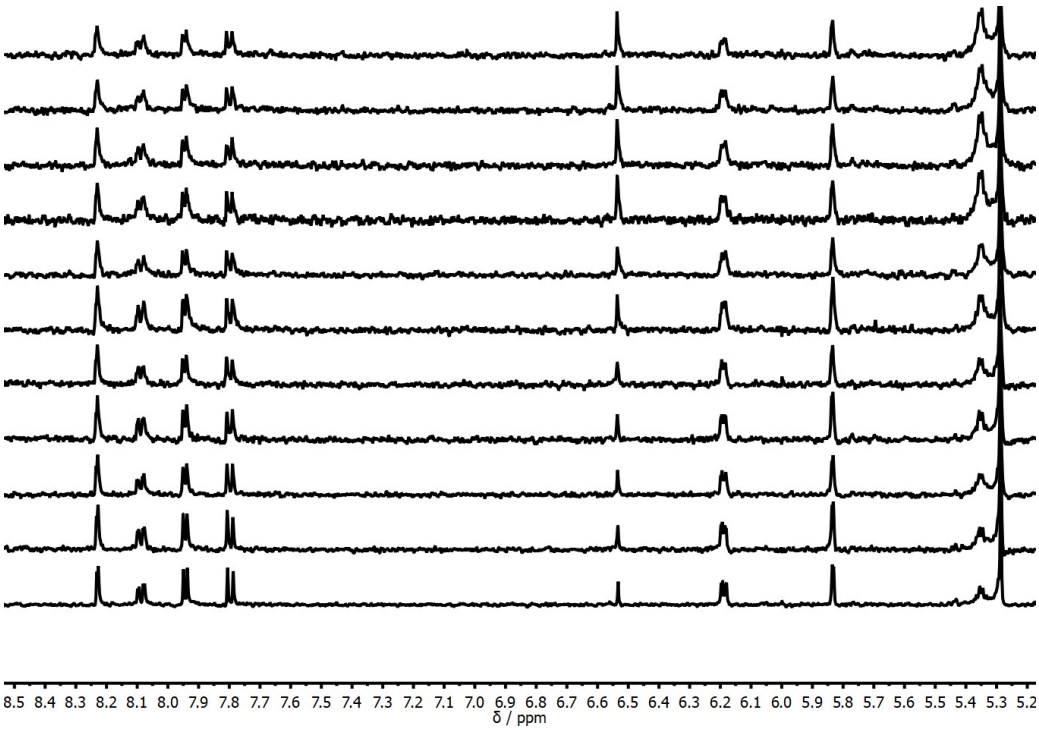

Figure S.64 – Stack plot for the NMR dilution of **8** in *n*-octane with concentration ranging from 0.166 mM (bottom) to 0.0249 mM (top). Peaks at 5.35 and 6.30 ppm are impurities in the solvent.

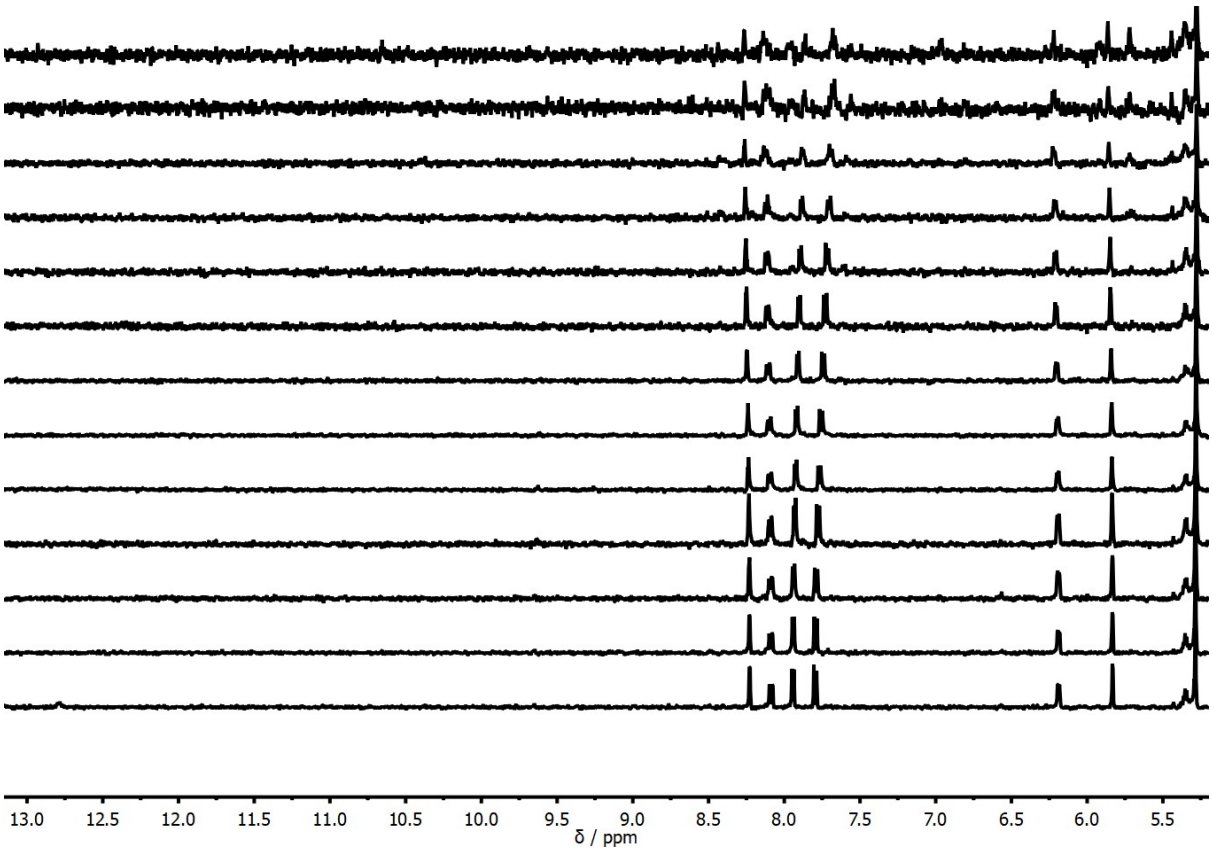

Figure S.65 – Stack plot for the NMR titration of PFTB into **8** (0.166 mM) in *n*-octane at 298 K. Peak at 5.30 ppm is an impurity in the solvent.

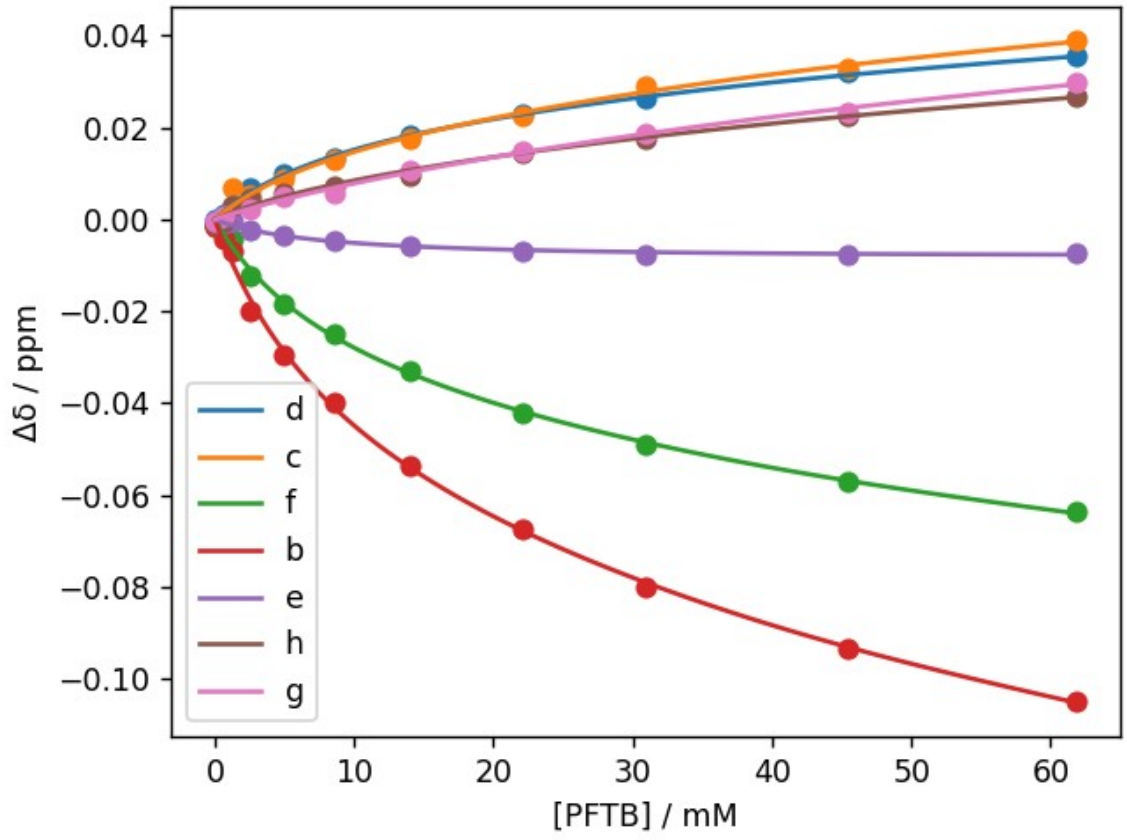

Figure S.66 – Fit for the NMR titration of PFTB into **8** (0.166 mM) to a 1:2 titration in *n*-octane at 298 K.

Results from fitting of PFTB titration data to a 1:2 binding isotherm

Compound	X	K_1 / M^{-1}	K_2 / M^{-1}
1	-	47 ± 7	4 ± 2
3	CN	46 ± 7	5 ± 2
4	CF_3	52 ± 12	12 ± 4
5	H	69 ± 11	14 ± 6
6	Me	76 ± 19	10 ± 6
7	OMe	92 ± 6	12 ± 8
8	NMe_2	123 ± 12	6 ± 9

Table S.1 – Association constants measured by UV/Vis absorption titrations (errors are quoted as two standard deviations based on at least three different experiments).

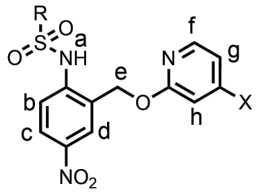

Figure S.67 – Structure of sulfonamides with proton labelling scheme.

The ^{1}H NMR titration data were fitted using a 1:2 binding isotherm with the values of K_1 and K_2 fixed at the values determined from the UV/vis titration. The UV/vis absorption data shows clear changes in direction at some wavelengths. These data do not fit to a 1:1 binding isotherm but fit well to a 1:2 isotherm, allowing reliable determination of K_1 and K_2. In contrast, none of the signals in the ^{1}H NMR titration data show a change in direction, which precludes reliable separation of the two binding events and accurate determination of K_1 and K_2. However, the complexation-induced changes in chemical shift could be accurately determined from the ^{1}H NMR data by fixing the known association constants from the UV/vis titration experiments and fitting the changes in chemical shift for the two binding events.

Compound	X	Δδ(a)	Δδ(b)	Δδ(c)	Δδ(d)	Δδ(e)	Δδ(f)	Δδ(g)	Δδ(h)
1	-	0.04	-0.05	0.02	0.01	-	-	-	-
3	CN	0.14	-0.06	0.02	0.03	0.00	0.00	0.02	0.02
4	CF_3	0.15	-0.05	0.00	0.01	-0.02	-0.02	0.00	0.00
5	H	0.29	-0.06	0.02	0.02	-0.01	-0.03	0.02	0.01
6	Me	0.36	-0.07	0.02	0.03	0.00	-0.03	0.03	0.01
7	OMe	-	-0.06	0.01	0.02	0.00	-0.02	0.01	0.01
8	NMe_2	-	-0.07	0.03	0.02	0.01	-0.04	0.01	0.01

Table S.2 – Complexation-induced changes in chemical for the first binding event. Protons e-h do not exist for compound **1** as the pyridyloxy group is replaced by a methyl group. For compounds **7** and **8**, the NH signal was not visible in the ^{1}H NMR spectrum.

Compound	X	Δδ(a)	Δδ(b)	Δδ(c)	Δδ(d)	Δδ(e)	Δδ(f)	Δδ(g)	Δδ(h)
1	-	0.18	-0.12	0.04	0.04	-	-	-	-
3	CN	0.04	-0.11	0.04	0.05	0.01	0.00	0.07	0.08
4	CF_3	0.38	-0.10	0.05	0.05	-0.01	-0.04	0.04	0.04
5	H	0.33	-0.08	0.03	0.04	0.00	-0.04	0.04	0.04
6	Me	0.19	-0.09	0.02	0.03	-0.01	-0.03	0.03	0.04
7	OMe	-	-0.10	0.05	0.04	-0.01	-0.05	0.05	0.05
8	NMe_2	-	-0.17	0.07	0.06	0.00	-0.10	0.08	0.07

Table S.3 – Complexation-induced changes in chemical relative to the free host for the second binding event. Protons e-h do not exist for compound **1** as the pyridyloxy group is replaced by a methyl group. For compounds **7** and **8**, the NH signal was not visible in the ^{1}H NMR spectrum.

X-ray diffraction

X-ray data were collected on a Bruker D8-QUEST diffractometer, equipped with an Incoatec IμS Cu microsource (λ = 1.5418 Å) and a PHOTON-III detector operating in shutterless mode. The crystal temperature was held at 180(2) K using an Oxford Cryosystems open-flow N2 Cryostream. The control and processing software was Bruker APEX4 (ver. 2021.4-0). Structures were solved using SHELXT[3] and refined using SHELXL.[4]

Structure **3** (displacement ellipsoids at 50% probability):

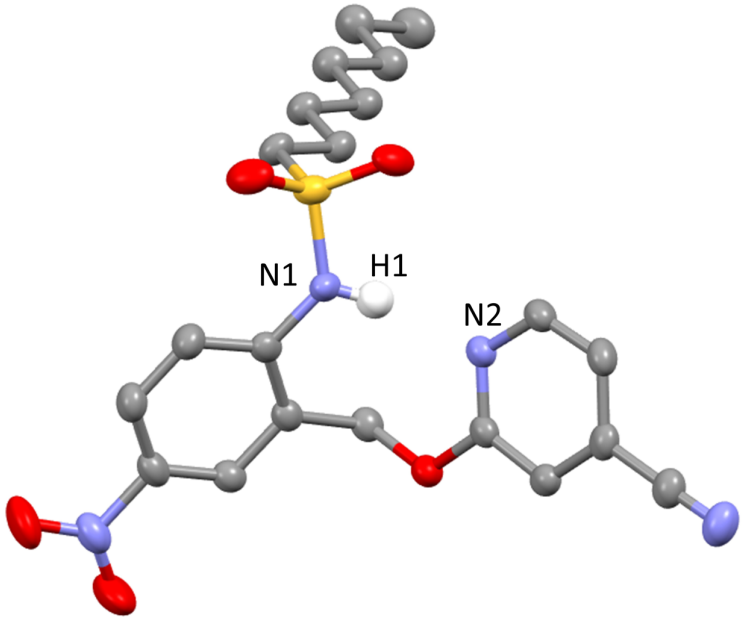

Figure S.68 – Crystal structure of compound **3** determined by X-ray diffraction. Ellipsoids at 50% probability.

D	H	A	D-H (Å)	H···A (Å)	D···A (Å)	D-H···A (°)
N1	H1	N2	0.857	1.945	2.778	163.33

Table S.4 – Measurement of distances and angles involved in the intramolecular H-bond in compound **3**.

Cambridge Identification code	CH_B1_0070
Chemical formula	$C_{21}H_{26}N_4O_5S$
Formula weight	446.52
Temperature / K	180(2)
Crystal system	Monoclinic
Space group	$P2_{1/C}$
a / Å	5.6438(2)
b / Å	35.5926(12)
c / Å	11.0653(4)
α / °	90
β / °	95.787(2)
γ / °	90
Volume / $Å^3$	2211.44(13)
Z	4
Density (calculated) / g cm^{-3}	1.341
Absorption coefficient / mm^{-1}	1.644

F(000)	944
Crystal size / mm^3	0.240 x 0.060 x0.040
2-theta range / °	5.482 to 66.552
Index ranges	-6<=h<=6, -42<=k<=42, -13<=l<=13
No. of reflections collected	40491
No. of independent reflections	3896
R(int)	0.0495
Completeness to theta = 66.552°	99.7 %
Absorption correction	Semi-empirical from equivalents
Max. and min. transmission	0.7528 and 0.5926
Refinement method	Full-matric least squares on F^2
No. of parameters / restraints	285 / 0
Goodness-of-fit on F^2	1.032
Final R indices [I>2sigma(I)]	R1 = 0.0326, wR2 = 0.0796
R indices (all data)	R1 = 0.0378, wR2 = 0.0835
Largest diff. peak and hole	0.211 and -0.360

Table S.5 – Summary of the crystal and refinement details.

References

1. Fulmer, G.R., Miller, A.J.M., Sherden, N.H., Gottlieb, H.E., Nudelman, A., Stoltz, B.M., Bercaw, J.E., Goldberg, K.I., *Organometallics,* **2010**, 29, 2176-2179
2. Hanna, F. E., Root, A. J., Hunter, C. A., *Chem. Sci.*, **2023**, 14, 11151–11157
3. Sheldrick, G. M., *Acta Cryst. Sect. A*, **2015**, 71, 3-8
4. Sheldrick, G. M., *Acta Cryst. Sect. C*, **2015**, 71, 3-8